CR-184284

FINAL PROJECT REPORT

National Aeronautics and Space Administration
Contract NAS8-37141
Universities Space Research Association
Subcontract 3473-01.

Model Studies on the Role of Moist Convection as a Mechanism for Interaction Between the Mesoscales

PREPARED FOR :

Dr. Michael W. Kalb
Universities Space Research Association
4950 Corporate Drive
Suite 100
Huntsville, AL 35806

PREPARED BY :

MESO, Inc.
185 Jordan Road
Troy, NY 12180

July 22, 1991

TABLE OF CONTENTS

Model Studies on the Role of Moist Convection as a Mechanism for Interaction Between the Mesoscales

KENNETH T. WAIGHT III, J. AARON SONG, JOHN W. ZACK AND PAMELA E. PRICE

Mesoscale Environmental Simulations and Operations, Inc., 185 Jordan Road, Troy, NY 12180

ABSTRACT

A three year research effort is described which had as its goal the development of techniques to improve the numerical prediction of cumulus convection on the meso-β and meso-γ scales. Two MESO models are used, the MASS (mesoscale) and TASS (cloud scale) models. The primary meteorological situation studied is the June 28-29, 1986 COHMEX case study, in which significant mesoscale precipitation occurred over the COHMEX study area on a day with relatively weak large scale forcing.

The problem of determining where and when convection should be initiated is considered to be a major problem of current approaches. Assimilation of moisture data from satellite, radar and surface data is shown to significantly improve mesoscale simulations. The TASS model is shown to reproduce some observed mesoscale features when initialized with 3-D observational data. Convective evolution studies center on comparison of the Kuo and Fritsch-Chappell cumulus parameterization schemes to each other, and to cloud model results. The Fritsch-Chappell scheme is found to be superior at about 30 km resolution, while the Kuo scheme does surprisingly well in simulating convection down to 10 km in cases where convergence features are well-resolved by the model grid. Results from MASS-TASS interaction experiments are presented and discussed. A discussion of the future of convective simulation is given, with the conclusion that significant progress is possible on several fronts in the next few years.

---

1. Introduction

Cumulus convection occurs routinely over large portions of the globe, greatly affecting daily human activities. In addition to the deadly threat of exceptionally severe thunderstorms with tornadoes and flash flooding, large numbers of deaths and substantial property damage result from ordinary convection in the form of lightning, localized flooding, downbursts and straight line winds. Despite this, operational numerical prediction of convection is very poor compared to forecasting of other significant weather events such as winter storms. Fig. 1 shows the annual trend of operational forecast skill by the U.S. National Meteorological Center (NMC) as measured by THREAT score, a method commonly used for Quantitative Precipitation Forecast (QPF) verification. For each of the four types of forecasts, the worst performance occurs in the summertime months, when cumulus convection

is the dominant precipitation mechanism.

One of the fundamental difficulties encountered in simulating convection is that a wide range of length scales is involved. Convection is often associated with large scale (1000-10000 km) atmospheric wave motions and may be organized into meso-β scale circulations (20-200 km), and yet complex motions occur inside individual clouds (100 m-1 km). In addition, important microphysical processes which occur on even smaller scales cannot be neglected. Two traditional methods of studying convection have been employed. First, hydrostatic models from the global to meso-β scale have treated convection **implicitly**, by attempting to parameterize convection as a subgrid scale process. Many basic parameterization questions have not yet been settled, most related to the lack of a clear scale separation, especially for meso-β models, between what processes should be resolved on the model grid and what should be considered subgrid scale. A more fundamental problem is that convection may be simply too complex to be approximated by any single parameterization scheme. Second, three-dimensional cloud models treat convection **explicitly**, attempting to resolve the spectrum of convective motions with a grid spacing generally less than 1000 m, on the order of the size of individual cumulus updrafts. Sophisticated cloud microphysical equations are included for a large set of hydrometeor interactions. Because of the very large computational resources they consume, cloud models suffer from small domain sizes (typically less 200 x 200 km), which effectively eliminate interaction with the important larger scales of motion.

The major objective of this research effort has been to improve the treatment of convection in mesoscale numerical models. The fundamental method chosen has been to combine the implicit and explicit approaches by using two state-of-the-art MESO models, the Mesoscale Atmospheric Simulation System (MASS), and the Terminal Area Simulation System (TASS). The approach of this project has been to investigate the convective simulation problem by first improving various aspects of the implicit (mesoscale model and parameterization schemes) and explicit (cloud model) treatments separately, and then to combine the two models in order to concentrate on what is considered the most difficult problem, the complex interaction between individual convective elements and their meso-β-scale environment.

The problem of convective simulation may be separated into two components: **initiation** and **evolution**. For both the implicit and explicit approaches, convective evolution seems to have received the most attention. Much of the development of cumulus parameterization schemes for mesoscale models has centered on properly estimating the vertical profiles of convective heating, moistening and momentum

tendencies. The cases used in previous studies have tended to be ones for which the forcing mechanism was well-resolved by the model grid, so that the question of exactly where and when convection should have been initiated across the domain was not carefully examined. Analogously, the large majority of cloud modeling studies have employed impulses of heat or momentum to initiate convection with the intent of investigating cloud evolution, avoiding the question of actual initiation.

The results in this report are organized into three sections. Section 2 summarizes research performed regarding convective initiation, using the mesoscale and cloud models separately. Section 3 similarly presents results from both models dealing with convective evolution. Section 4 then presents the results of model interaction studies. In addition, Section 5 concludes the project by discussing the possible future directions of convective simulation.

1.1 MASS Description

MASS combines a data preprocessor with a mesoscale model. The preprocessor is a set of FORTRAN programs which prepares initial and lateral boundary conditions for subsequent model simulations. The programs perform the data processing, horizontal and vertical interpolation, and objective analyses necessary to transform various forms of meteorological data into model-ready datasets.

The MASS model (Kaplan *et al.*, 1982) is a hydrostatic, three-dimensional mesoscale model which integrates the primitive equations to predict the two horizontal velocity components, temperature, water vapor mixing ratio and surface pressure. The model uses the terrain-following normalized pressure (sigma) vertical coordinate system. The model contains two well-known cumulus parameterization schemes, the Kuo scheme (Kuo, 1965, 1974; Anthes, 1977a) and the Fritsch-Chappell scheme (Fritsch and Chappell, 1980).

1.2 TASS Description

The three-dimensional TASS cloud model is nonhydrostatic and compressible with prognostic equations for momentum, potential temperature, pressure and six bulk water categories: water vapor, cloud droplets, ice crystals, rain, snow and graupel/hail. It includes a complex microphysical parameterization scheme following Lin *et al.* (1983) and Rutledge and Hobbs (1983). For details on the model formulation, see Proctor (1987a). Verification tests of the model have been completed for several different types of convection, from weak multicellular Florida convection to long-lasting supercell hailstorms, with successful results (Proctor, 1987b). In addition, the model has recently been applied to the simulation of mountain-forced wave evolution using initialization from a high-resolution MASS mesoscale simulation.

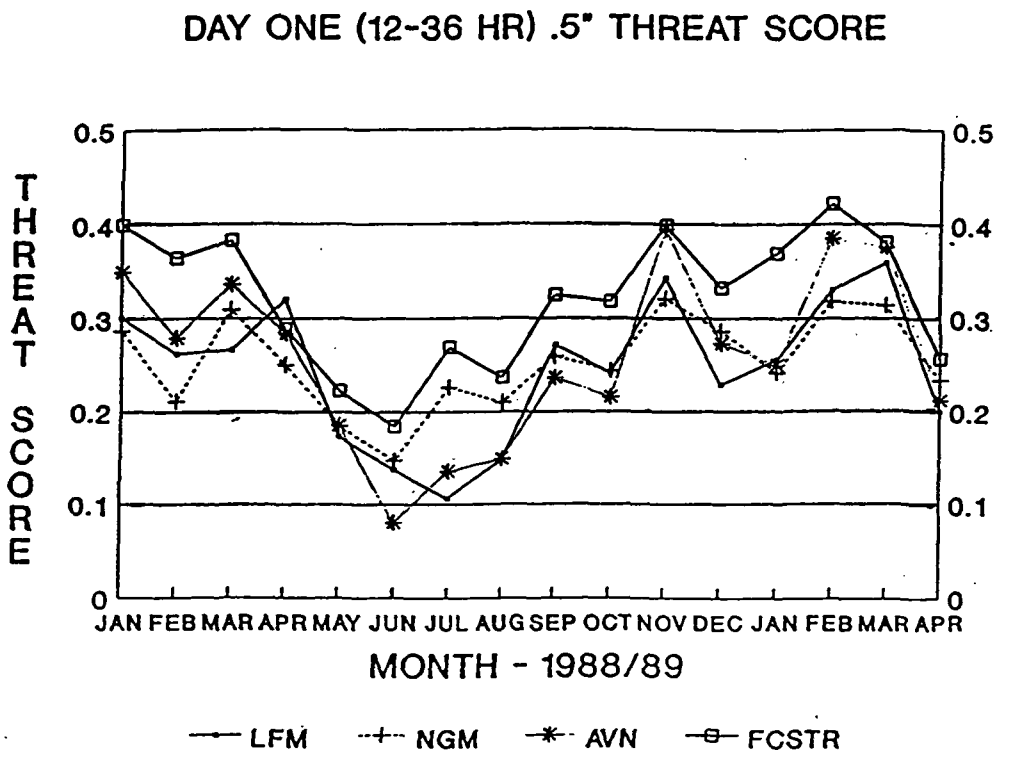

Figure 1 Annual trend of THREAT scores for four types of NMC forecasts for a period in 1988 and 1989. A THREAT score of one is perfect, while a value of zero indicates no predictive skill. From Mostek and Junker (1989).

2. The Problem of Convective Initiation

The relative importance of initiation and evolution depends mostly on one's immediate goal in running a simulation. If the purpose is to study a particular convective event or type of event in order to better understand its structure and evolution (research mode), then a poorly simulated distribution of convection outside of the area of interest is of relatively little concern. If, on the other hand, the purpose is to successfully predict the location and timing of convection in real time (operational mode), then the ability of the scheme to initiate convection correctly becomes a necessity. Since meso-β-scale models currently exist almost exclusively in the research environment, and have mostly been used for case studies where the focus is on one particular feature or storm, very little has been done, for instance, to quantitatively verify the ability of current convective parameterization schemes to predict the spatial and temporal distribution of convection.

A substantial portion of the initiation problem is caused by inadequate knowledge of the characteristics of the earth's surface (soil moisture, surface albedo, vegetation, etc.) and of the three-dimensional structure of the atmosphere. Mesoscale models cannot possibly forecast the evolution of convection correctly if the data used in the model initialization misses important features such as convergence or moisture gradients. Even given "perfect" model initial conditions however, currently available cumulus parameterization schemes would predict significantly different distributions of convection due to their very different criteria for convective initiation. Fritsch and Chappell (1980) presented a scheme intended for meso-β-scale models which has shown considerable skill in simulating midlatitude warm season convective systems (Zhang and Fritsch, 1986a; Zhang and Fritsch, 1988; Zhang *et al.*, 1989). Convection begins at a grid point in this scheme if a parcel raised to its lifting condensation level (LCL) is positively buoyant (*i.e.* if there is available buoyant energy), and if a one-dimensional cloud model is subsequently able to form a cloud of sufficient depth above the LCL. In addition, the mesoscale (grid-resolvable) vertical velocity at the LCL exerts a strong role through a special temperature perturbation term which is added to the temperature of the lifted parcel. Frank and Cohen (1987) have formulated a meso-β scale scheme which defines threshold amounts of both low level mass convergence and latent instability as being necessary conditions for the occurrence of convection. Anthes (1977a) presents a scheme following Kuo (1965, 1974) which also requires grid scale convergence. The difference in the two types of closure assumptions is subtle but important. For the Fritsch-Chappell scheme, mesoscale vertical velocity is a contributing factor but not a necessary condition. Convection could occur without

any dynamic forcing for a sufficiently unstable sounding. The Frank-Cohen scheme (originally intended for tropical application) and the Kuo-type schemes require the presence of mesoscale convergence. In each case, the two controlling factors are thermodynamic instability and mesoscale dynamic forcing (mass convergence or hydrostatic vertical velocity). However, the relative importance of these two factors for different types of initiation mechanisms is not at all clear.

Cooper *et al.* (1982) studied sea breeze convection over South Florida and found that convergence on two scales were involved in convective initiation. First, a peninsular scale convergence was related to the sea breeze circulation which occurred with regularity. This convergence triggered thunderstorms beginning in the late morning. Second, outflows from the original convection generated convergence on smaller scales and often initiated new convection.

It is also possible that other parameters could be useful in predicting the location of convective initiation, such as a measure of the subgrid scale inhomogeneity of the earth's surface, or some indicator of the state of the planetary boundary layer which could represent the vigor and variability of rising thermals. Chen and Orville (1980) found that mesoscale convergence weakened an inhibiting temperature inversion and moistened the lower atmosphere in a two-dimensional cloud model simulation, leading to stronger thermals and deeper convection. Balaji and Clark (1988) and Redelsperger and Clark (1990) have investigated the interactions between boundary layer instabilities and the formation of deep convection.

In addition, the dependence of any initiation criterion on model grid size is very poorly understood. It is believed that a significant improvement in the definition of criteria for the initiation of deep convection by a cumulus parameterization scheme would result in a substantial improvement in the ability of a mesoscale model to correctly simulate the timing and location of warm season precipitation.

A great deal of resources were used to attack the convective initiation problem with both the mesoscale and cloud models. In the following subsections, this research is summarized. Early in the project, a case from the COoperative Huntsville Meteorological EXperiment (COHMEX), June 28-29, 1986, was selected as a good candidate for both mesoscale and cloud scale research, mostly because of the extensive observations taken on that day, including three-hour meso-β network rawinsondes. Section 2.1 briefly describes that case. Section 2.2 chronicles the protracted effort to produce a June 28 MASS simulation which accurately initiates observed convection. Section 2.3 summarizes a TASS June 28 simulation in which three-dimensional initial conditions were used instead of the thermal bubble initiation technique. Section 2.4 presents results from a TASS simulation over Florida which used a realistically-varying pattern of surface sensible and latent heat

fluxes to initiate convection.

2.1 June 28-29, 1986: The Case That Wouldn't Die

A complex series of precipitation events occurred on June 28-29, 1986 during COHMEX. A more detailed description of the experimental platform of COHMEX and the general weather conditions is given in Williams *et al.* (1987), while Knupp and Williams (1988) provide a qualitative analysis of this particular case. The event of main interest was a small mesoscale convective system which formed about 1900 UTC 28 June over western Tennessee and moved eastward through the afternoon into the network of COHMEX rawinsonde sites, producing locally heavy (40 mm) rainfall. This kind of system is seen as typical of warm season precipitation events in the presence of relatively weak large scale forcing which may be responsible for locally significant weather, yet is almost never predicted. As such, it provides a challenge to the ability of current mesoscale models to initiate convection in the right place and at the right time.

Fig. 2 shows manually digitized national radar summaries at three hour intervals between 1200 UTC 28 June and 0000 UTC 29 June, spanning the period of greatest interest. At 1200 UTC, precipitation is occurring in Arkansas and Mississippi associated with substantial low level moisture from the remnants of Hurricane Bonnie. At about 1900 UTC, a small convective system is formed north of Memphis, TN, presumably related to differential surface heating at the western edge of an area of low to mid level cloudiness in central Tennessee. The system propagates eastward during the following twelve hours. As it moves into the COHMEX mesonetwork, convective cells on the western edge of the network weakened and evolved into a region of stratiform precipitation, while a new group of cells were initiated in the center of the network (Fig. 3).

2.2 The Quest for an Ideal MASS June 28 Simulation, or
A Funny Thing Happened on the Way to MASS-TASS Coupling

The original idea of simulating the COHMEX case was that once MASS had successfully simulated the events of June 28, the most important research would involve coupled MASS-TASS simulations which could be rigorously compared to high resolution COHMEX observations. What happened instead was that despite a great deal of effort, a completely successful mesoscale simulation was never achieved. For a case such as June 28, which is not strongly forced and organized by well-resolved meso-α or larger scale features, the initiation of convection in various parts of the domain is likely to be due to relatively subtle mesoscale features such as differential surface fluxes of heat and moisture, local terrain effects, or interaction with outflow boundaries from previous convection. These features are usually not

well resolved by conventional observations.

Although COHMEX observations were extensive on both the meso-β and meso-γ scales within the network of special rawinsonde sites, the primary June 28 convection had its beginning in a system which formed well outside the network in western Tennessee, so that no special COHMEX observations could help to resolve the forcing for the original initiation event. Instead, efforts centered on using additional observations, such as standard surface aviation reports, GOES satellite data, digitized radar data and cooperative precipitation reports.

June 28 MASS simulations generally consisted of a 36 hr large scale run initialized at 0000 UTC 28 June with a resolution of 75 km, covering most of the eastern half of the U.S. Then at 1200 UTC 28 June, model fields were used as a first guess for another initialization with new 1200 UTC data. This second initialization was done on a 37.5 km grid nested within the large mesh. A 12 or 24 hr nested simulation using time-dependent lateral boundary conditions taken from the large mesh run was then carried out. Most of the discussion below concerns the 37.5 km nested simulations.

Archived surface aviation reports were obtained from the National Climatic Data Center (NCDC) in Asheville, NC and code was written to ingest it into the MASS model initial state. The inclusion of surface data slightly improved the simulations by significantly altering the low level fields. For the 0000 UTC 28 June large mesh initialization, the main result was to make the COHMEX area somewhat cooler and drier at the surface, resulting in a beneficial reduction in the amount of convection in the whole region compared to the corresponding run without surface data. For the nested run, the reinitialization with surface data results in warmer initial surface temperature in the COHMEX area (generally by about 5°C) and slightly decreased dew points (1-2 °C).

Since convective simulations have been shown to often be quite sensitive to the initial moisture field (Zhang and Fritsch, 1986b), an algorithm was developed to assimilate moisture information in the form of GOES infrared and visible satellite digital data, surface aviation reports of cloud base height, and manually digitized radar data. The algorithm builds on the work of Zack *et al.* (1988) and resembles the methods of Wolcott and Warner (1981), Ninomiya and Kurihara (1987), and Wang and Warner (1988). The four sources of data act in combination to modify MASS's initial water vapor field. The cloud base height is taken from nearby cloud base height estimates, the cloud top height is inferred from GOES infrared temperatures, and clear and cloudy areas are distinguished from GOES visible brightness values. In areas with radar echoes above a threshold intensity, the relative humidity from cloud top to the ground is increased to nearly saturation. The method is partially described in Waight *et al.* (1989). These data sources are used to provide estimates

of the cloud fraction (from zero to one) at each satellite pixel in an arbitrary number of vertical layers. The cloud fractions are averaged to the model grid boxes (there typically are many satellite pixels per grid box) and then converted to relative humidity by inverting a set of relative humidity (RH)-cloud fraction relationships of the type used in many models to estimate cloud effects from a given moisture field. These synthetic RH profiles are then merged with a conventional RH analysis to produce a revised initial model relative humidity field. Improvements are anticipated in two areas:

(1) The initial distribution of model cloudiness should be far more realistic (mesoscale detail, sharp cloud boundaries), resulting in a better representation of radiative processes (*e.g.* differential heating leading to an inland sea breeze).
(2) Significantly moistening areas with known precipitation at the initial time (where there are radar echoes) should result in a decrease in the time required by the model to generate that precipitation (*i.e.* reduce the "spin-up" time).

The assimilation does result in significant changes to the moisture field, leading to changes in the June 28 simulation. Fig. 4 shows the four sources of synthetic moisture data at 1200 UTC 28 June which were used in the moisture assimilation scheme. Fig. 5 shows the low level relative humidity field (directly related to cloud fraction in the MASS model) without (Fig. 5a) and with (Fig. 5b) the complete moisture assimilation. The moisture gradients are very sharp, unlike rawinsonde-derived fields which tend to be smooth. The additional moisture information led to an overall qualitative improvement in the simulated precipitation patterns, but results were poorer in some geographical areas. Two major changes resulting from the moisture enhancement follow:

(1) One hour into the moisture-enhanced simulation, convective precipitation areas in Arkansas developed in the vicinity of observed 1200 UTC radar echoes, where moisture was added by the scheme. The scheme successfully reduced the precipitation spin-up time in that area.
(2) A persistent deficiency in the June 28 simulations has been the difficulty in reproducing the heavy precipitation observed in Louisiana and southwestern Arkansas associated with the remnants of Hurricane Bonnie. The moisture enhancement scheme actually decreased the amount of convection there by drying and stabilizing

western Louisiana because the area was clear in the visible satellite imagery.

All of the runs discussed so far contained no variation in surface characteristics (albedo, roughness length, etc.) Since gradients of soil moisture have been shown by other investigators to be significant in some cases (Ookouchi *et al.*, 1984; Lanicci *et al.*, 1987; Chang and Wetzel, 1991), an attempt was made to improve the simulation by the use of archived surface hourly rainfall measurements taken by the U.S. network of cooperative observers, acquired from NCDC. After interpolating the point observations to the MASS grid, the Antecedent Precipitation Index (API) method (see, for example, Chang and Wetzel, 1991) was used to infer a soil moisture distribution based on measured precipitation for a 31-day period preceding the initialization time. Fig. 6 shows precipitation observations for the two 24-hr periods prior to 1200 UTC 28 June. The major feature relevant to the case is the very heavy (over 100 mm in several places) precipitation generated by Hurricane Bonnie as it moved northward along the Texas-Louisiana border into Arkansas. When the API-based soil moisture field was introduced into MASS, the results differed strongly only in the areas of very high soil moisture, where convection was suppressed, contrary to observations. The reason for the lack of convection is that the wet soil resulted in weaker surface sensible heat fluxes as more of the incoming radiative energy went toward evapotranspiration. Controlled tests of the simulation's sensitivity to initial soil moisture show that a moderate value (0.4 uniformly across the domain) produces convection in the area, while very low (0.05) or very high (0.8) values do not. It appears that increasing soil moisture produced two competing effects: lower temperatures and increased dew points.

After much travail, the best June 28 simulation employed the full moisture assimilation scheme but used a constant initial soil moisture of 0.4. The run, shown in Fig. 7, was quite good in several respects. An initial low level dew point maximum was centered over western Tennessee, resulting in a minimum in the lifted index field. As a result, a convective system formed at approximately the right location, although it was several hours too early (Fig. 7a). The system propagated eastward at the correct speed, and dissipated over the COHMEX network (Fig. 7b-d). The central Tennessee convection did not, however, intensify just before 0000 UTC 29 June as observed, and there was still too little convection in Louisiana. The overall pattern of convection over the entire domain was reasonably similar to what was observed (Fig. 2), even at 0000 UTC 29 June, after twelve hours of simulation. This represents a substantial qualitative improvement over runs without moisture assimilation.

The conclusion from this series of moisture-adjusted runs is that while it is possible to substantially improve a simulation with moisture assimilation, the

addition of new sources of data tends to improve the simulation in some ways at the same time that it degrades it in others. *The lesson is that for a successful convective simulation of a case with weak large scale forcing, many subtle things need to be done well on a variety of scales simultaneously.*

2.3 Banning the Bubble: TASS 3-D June 28 Initialization Simulations

The storm initiation problem involves atmospheric spatial scales which are shorter than the organizing hydrostatic scales of motion responsible for producing a moist convectively unstable environment, *i.e.* ~10 km and temporal scales of minutes. With the recent advances of computer speed, such meso-γ scale dynamical pre-convective cloud scale processes involving convective "triggering" are beginning to be incorporated, with various degrees of simplification, into numerical simulations which explicitly resolve deep convection. For example, Crook *et al.* (1990), in simulating the regeneration of a nocturnal squall line which is described in detail in Carbone *et al.* (1990), considered three types of regeneration mechanisms which are all associated with horizontal gradients in the upstream environment. Among them, they found that an increase of low level moisture and increase of low level shear following a gust front (*i.e.* in a Lagrangian framework moving with the gust front) are both able to lower the level of free convection (LFC) and/or increase the lifting at the gust front thereby enhancing the convective regeneration. Redelsperger and Clark (1990) found that the spatial organization of the simulated clouds (*i.e.* scale selection of convection) is determined primarily by the magnitude and direction of the shear in the zone spanning the boundary layer eddies and the overlying quasi-stationary gravity waves. Strong directional shear results in more banded (or two-dimensional) cloud structure, while speed shear results in more scattered (or three-dimensional) structure. Dynamically, the shear itself is maintained through a balance between the shear destruction by boundary layer mixing and shear production by a differential heating on a gentle slope. Tripoli and Cotton (1989a, 1989b) described a complete life cycle of the interactions among atmospheric processes of horizontal scales ranging from cumulus clouds to large scale mountain-plain solenoidal circulations. In simulating the Big Thompson storm, Yoshizaki and Ogura (1988) found that an essential dynamic factor of generating the observed heavy precipitation is the incorporation of a horizontally varying moisture field in association with the local orography.

A common similarity among these studies is that all of them include convectively explicit simulations (Schlesinger, 1982) initialized with an environment that is characterized by horizontal gradients in physical fields near the onset of convection. These include gradients of terrain heights, gradients of surface moisture or solar heating, or other gradients associated with the surface

"boundaries". As discussed in Balaji and Clark (1988), such a convective simulation initialization (or the "near-field" treatment) recognizes localized forcing, such as surface energy fluxes, as effective triggering mechanisms for deep convection. Convective initialization of this type is in contrast to those used when the mature stage convective processes (Klemp *et al.*, 1981) or convective-stratiform interactions (Lafore and Moncrieff, 1989) are the main focus. That is, if only the mature stage is of interest, or if a large scale property (such as a strong horizontally-uniformly shear in the lower troposphere) is known to dominate the storm dynamics, the use of a simple "bubble" (Schlesinger, 1982; Proctor, 1987b) has been a common way of initializing convective simulations. Due to data and computer limitations, however, the incorporation of realistic environmental gradients into convective simulations requires simplification of the environmental forcing. For instance, the above cited studies are essentially all restricted to two-dimensional models. Clearly, the simplification of considering only two-dimensional flow implies that a certain environmental realism is lost. There has not been, to the knowledge of the authors, studies utilizing convectively explicit simulations which are initialized with realistic environmental forcing in which the three-dimensional structure of both winds and thermodynamic fields are retained. In the current study, an attempt was made to illustrate a "first trial" of such a type of numerical simulation by utilizing a special observational dataset. Specifically , the goal of this study is to understand how exactly an observed convective initiation and its early-stage spatial organization is generated over a horizontal area of 200 km across, by using a convectively explicit simulation approach which, as an unavoidable limitation, uses a horizontal grid spacing of 3 km.

A TASS simulation of the June 28 case was initialized with three-dimensional data taken from COHMEX observations, mainly meso-β rawinsonde soundings. The COHMEX observational network is shown in Fig. 8, along with a box indicating the TASS model domain. The period of interest is the multicell storm development from 2100 UTC 28 June to 0000 UTC 29 June depicted in Fig. 3 (from Nashville NWS radar) and also in Fig. 9 (from CP-4 Doppler radar located in Huntsville, AL). This storm produced a peak rainfall rate exceeding 100 mm hr^{-1} and a 24-hr accumulated rainfall which was the largest of the entire COHMEX. At 2100 UTC (Fig. 3a), several convective cells were located at the western edge of the COHMEX mesonet, near the Lexington, TN site (Fig. 8). These cells represented the mesoscale convective system which formed in western Tennessee and propagated westward across the state at the approximate speed of a weak upper level shortwave. Fig. 9 depicts the initiation of new cells near the center of the mesonet, aligned in a southwest-northeast direction, as the older cells to the west weakened and evolved into an area of stratiform precipitation. The following three stages of the target

convective initiation which the TASS simulation will attempt to reproduce are schematically shown in Fig. 9:

(1) The first cells developed near St. Joseph (Fig. 8), or around the network southwest corner, around 2130 UTC (Fig. 9a).
(2) Cells formed along a line extending generally southwest-northeast through St. Joseph by 2200 UTC (Fig. 9b).
(3) Those cells between St. Joseph and Columbia intensified and developed eastward or southeastward by 2330 UTC (Fig. 9c).

The major factor which organized convective initiation in this case was found to be a region of high moisture content in the lower atmosphere. Figs. 10a and 10b show relative humidity fields at 850 and 700 mb at 0000 UTC 29 June which are analyzed from meso-β rawinsonde observations. It is clearly seen that a band of moistening extended from the southwest corner toward the northeast at this time. Fig. 10c shows the moist static energy field and Fig. 10d shows the calculated horizontal distribution of lifting condensation level, which both reflect the same feature. This low level horizontal moisture distribution is associated with pre-convective southwesterly flow which tapped abundant upstream moisture producing a meso-β scale pattern of substantial observed convective potential.

Several cloud model simulations were conducted which were initialized with a three-dimensional dataset produced by an objective analysis of the 0000 UTC 29 June COHMEX meso-β rawinsonde data. To actually reproduce all the details of the four-dimensional convective-environmental interactions on the network scale leading to the correct locations and sizes of the observed initial cloud scale cells is clearly beyond the capability of a 3 km grid simulation with coarse initial data and no variation in surface forcing. Instead, only a small part of the observed convective initiation (during the period from 2130-2330 UTC) is taken as the goal of the numerical simulations.

First, a one hour control simulation was made using only rawinsonde data. Fig. 11 shows the model-produced radar reflectivity and wind fields for three times during the course of the control simulation. Several features of the simulated convective initiation correspond well to observations; the earliest model convection formed around the southwest corner, then tended to develop toward the northeast (see Fig. 3). On the other hand, the southwest corner convection remained strong and organized after one hour of development, which was not observed. Analysis of terms in the turbulent kinetic energy equation shows that spatially-varying turbulent plume intensities were produced due to the fact that plumes in the convectively-favored (moist) region had greater buoyancy. The more intense

plumes in the southwestern corner of the domain then rose to a lifting condensation level (LCL) which was lower (Fig. 10d) than in other regions, also because of the moist initial conditions. Therefore, the dry boundary layer turbulent plumes in the favored area reached saturation more quickly, forming clouds and initiating free convection. Convection was then initiated progressively later toward the northeast corner of the domain.

In order to see if there were surface features which contributed to the target convective initiation but were not picked up by the rawinsonde observations, a sensitivity simulation was made in which PAM (Portable Automated Mesonet) surface data at 2115 UTC replaced the lowest model level initial data. The PAM data provided a smoother thermodynamic field around the southwest corner with somewhat lower RH but similar moist static energy as compared with the sounding-derived data alone. Over the north central part of the domain, moist static energies were somewhat higher with the PAM data. Fig. 12 shows fields from this simulation which can be compared directly to Fig. 11 (control run). It is seen that the additional low level data did not produce any significant difference during the first 20 minutes but some noticeable differences during the later times. The differences were mainly the enhanced model reflectivities in the downstream area over the eastern one-third of the domain, but not with significantly different peak reflectivity values. The three stages illustrated in Fig. 9 were all qualitatively produced as in the control simulation.

Another sensitivity simulation was made which is otherwise exactly the same as the control simulation except that a 2°C temperature "bubble" was added to the lowest level at five points scattered around the domain. These bubbles were chosen to occupy only one grid point at one level, and were thus expected to be small enough to not alter the domain energy budgets. The purpose of this sensitivity simulation was only to see if the pre-convective thermodynamic pattern could be easily distorted by simply adding small temperature perturbations at randomly selected grid points. The results of this run showed that the velocity impulses due to the bubbles did not produce significant differences in the model results until the end of the one hour simulation. The differences were mainly the somewhat enhanced model reflectivities over the north central and eastern parts of the domain; the pattern of convective evolution was retained.

One final sensitivity test was made in which the full three-dimensional wind field was replaced by a simple vertical profile of wind, so that there were no horizontal variations. The point of this test was to examine the influence of the local cyclonic wind field (associated with a midlevel shortwave trough) on the model results. The effect of the removal of the 3-D wind field was to slightly decrease the amount of convective activity on the northeastern edge of the model convection, although the differences in reflectivity are not very significant.

The main conclusion of this study is that the pattern of convective initiation in the June 28 TASS simulation was controlled by the pattern of low level moist static energy . The results are discussed in greater detail in Song and Kaplan (1991), including the following points:

(1) Mesoscale boundary layer turbulence fueled by high values of low level moist static energy, and the low elevation of the lifting condensation level resulting from a very moist planetary boundary layer are the two crucial ingredients in generating the spatial organization of early stage convective development or convective triggering.
(2) Periods of 90 minutes are sufficient to allow the hydrostatic scales of motion to modify the distribution of moist static energy and low level relative humidity to result in a significant change in the pattern of convective initiation.
(3) The meso-γ scale variability of convective initiation patterns is discernible from the distribution of terms in the turbulent kinetic budget within the planetary boundary layer.
(4) Changing the surface moisture or the horizontal variability of the low-level wind field, or adding random temperature bubbles produced only minor changes in the position of the convective triggering.

2.4 Banning the Bubble II: Florida Differential Surface Heating Simulations

Continuing the effort to explicitly simulate convective initiation, MESO recently completed a Phase I Small Business Innovation Research (SBIR) project with the Air Force Office of Scientific Research. Since the results are directly relevant to this study (the SBIR topic idea originated in the USRA work), they will be briefly summarized here.

The TASS model was used to investigate the convective initiation process for an idealized case over central Florida where the forcing was provided by differential surface heating. The surface heating pattern was generated from high resolution land use data by making simple assumptions relating surface characteristics to particular land use types. A shortwave albedo and a Bowen ratio (ratio of surface sensible to latent heat flux) were estimated for major land use types appearing in the Florida domain, shown in Table 1. Fig. 13 shows the resulting complex pattern of surface sensible heat fluxes. A three hour cloud model simulation with 750 m horizontal grid spacing produced a complicated field of both shallow and

precipitating cumulus clouds which is visually very impressive (Fig. 14). Analysis of the results showed that in the first half of the run, localized differential surface sensible heating produced small areas of deep convection associated with surface land use features (*e.g.* contrast between urban areas and forest/wetlands). In the latter half of the simulation, mesoscale convergence developed due to the lateral boundary conditions, which acted as a boundary between the unheated air outside the domain and the heated surface inside. This provided a mesoscale organization (convergence advecting inward from the model boundaries and on the coastline) which was well resolved by a conventional measure of mesoscale moisture convergence. Fig. 15 shows the good correlation between vertically integrated moisture convergence and rainfall for 8.25 km boxes averaged from the 750 m TASS data. Similarly, Fig. 16 shows a good relationship between subgrid scale (TASS grid scale) low level convergence and rainfall. TASS produced realistic convective initiation and evolution when forced by realistically complex surface forcing.

These results, taken together with the COHMEX 3-D initial data TASS simulations, demonstrate convincingly that the use of a nonhydrostatic model can be an excellent way to explicitly study the process of convective initiation. The initiation process can be directly simulated, without the necessity of a bubble. The knowledge obtained from analysis of cloud model simulations may then be incorporated into an improved mesoscale parameterization scheme. The mesoscale analysis of the Florida run (Figs. 15 and 16) encourages the idea that a simple mesoscale variable such as moisture convergence, possibly in combination with an inferred measure of subgrid scale forcing, can be useful in a successful parameterization scheme, even at the low end of the meso-β scale (about 10 km). Moisture convergence may prove to be an effective closure assumption relating convective precipitation rates to model resolved variables, while subgrid scale convergence may be an effective initiation criterion.

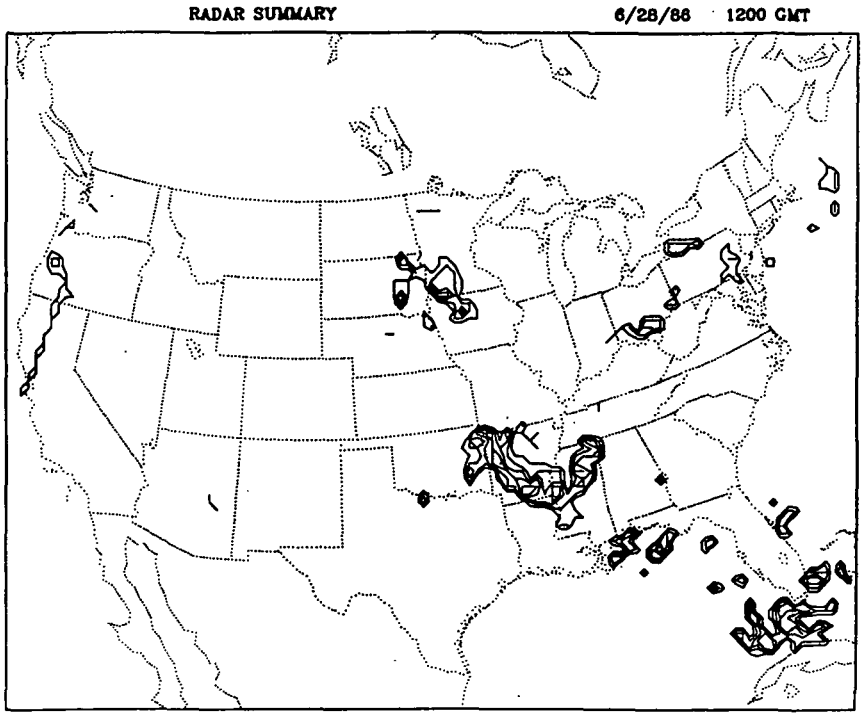

A

Figure 2 Manually-digitized radar summaries for (a) 1200 UTC 28 June 1986, (b) 1500 UTC, (c) 1800 UTC, (d) 2100 UTC and (e) 0000 UTC 29 June. Each contour represents one radar VIP level. The echoes in central Tennessee were the subject of COHMEX interest.

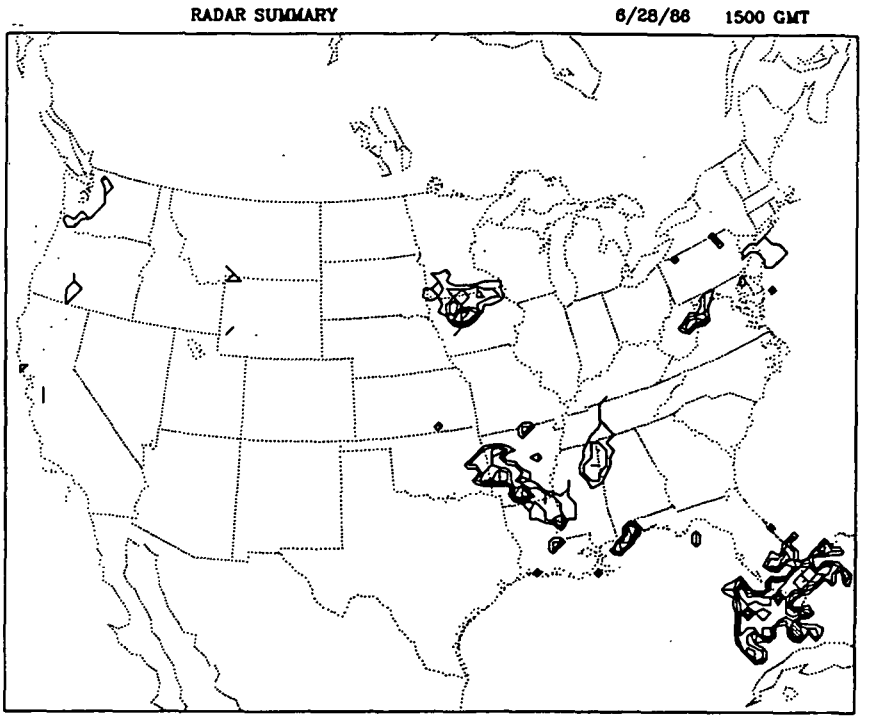

B

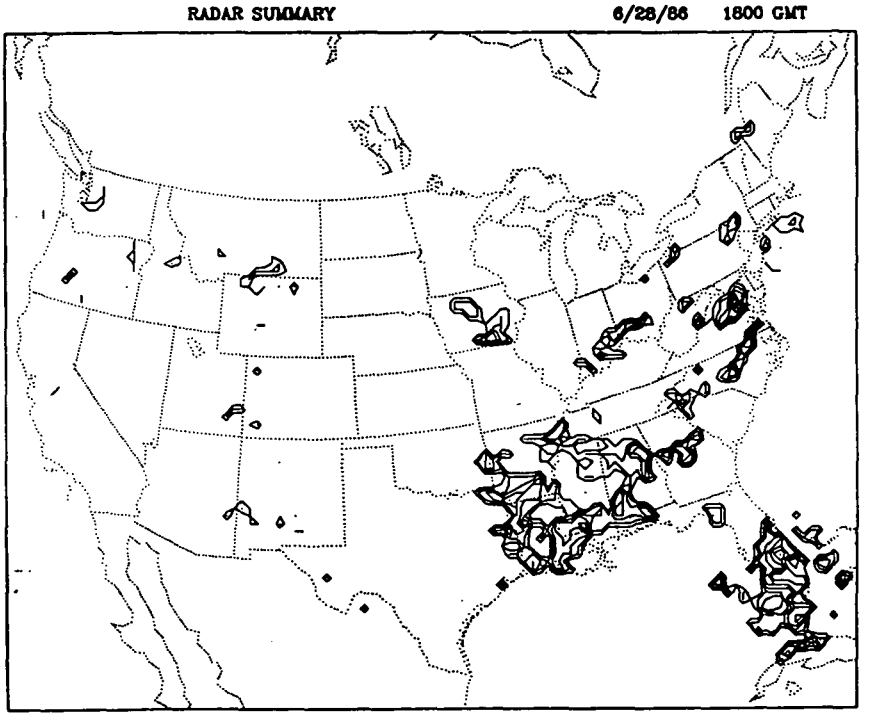

C

Figure 2 (continued)

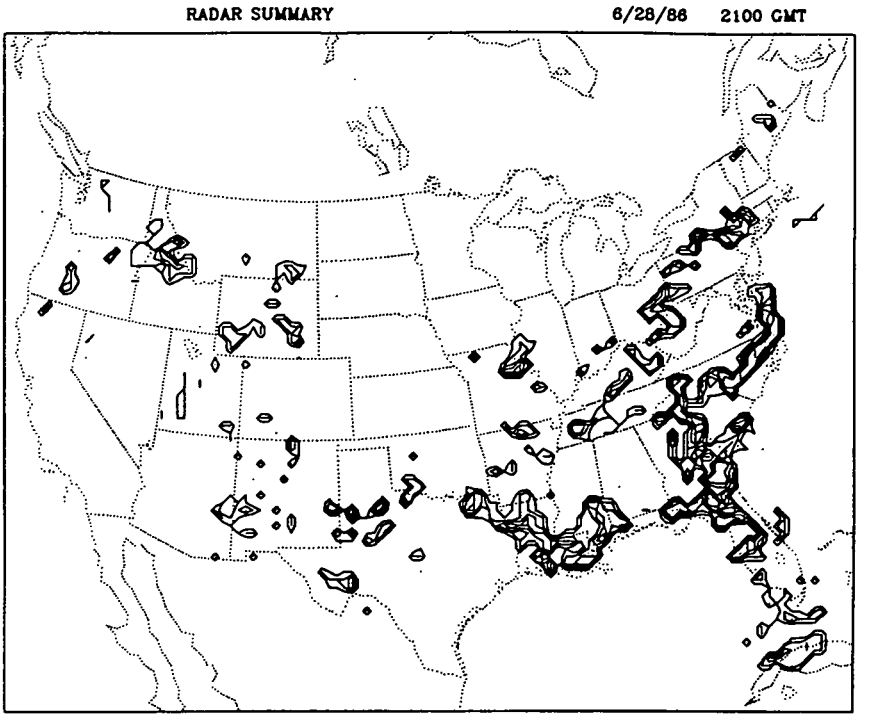

D

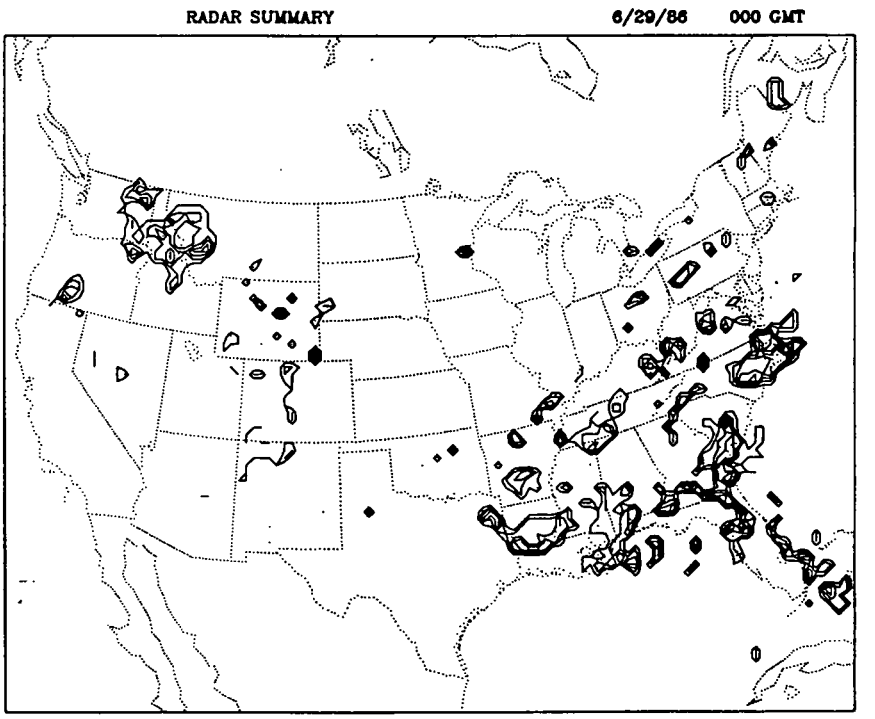

E

Figure 2 (continued)

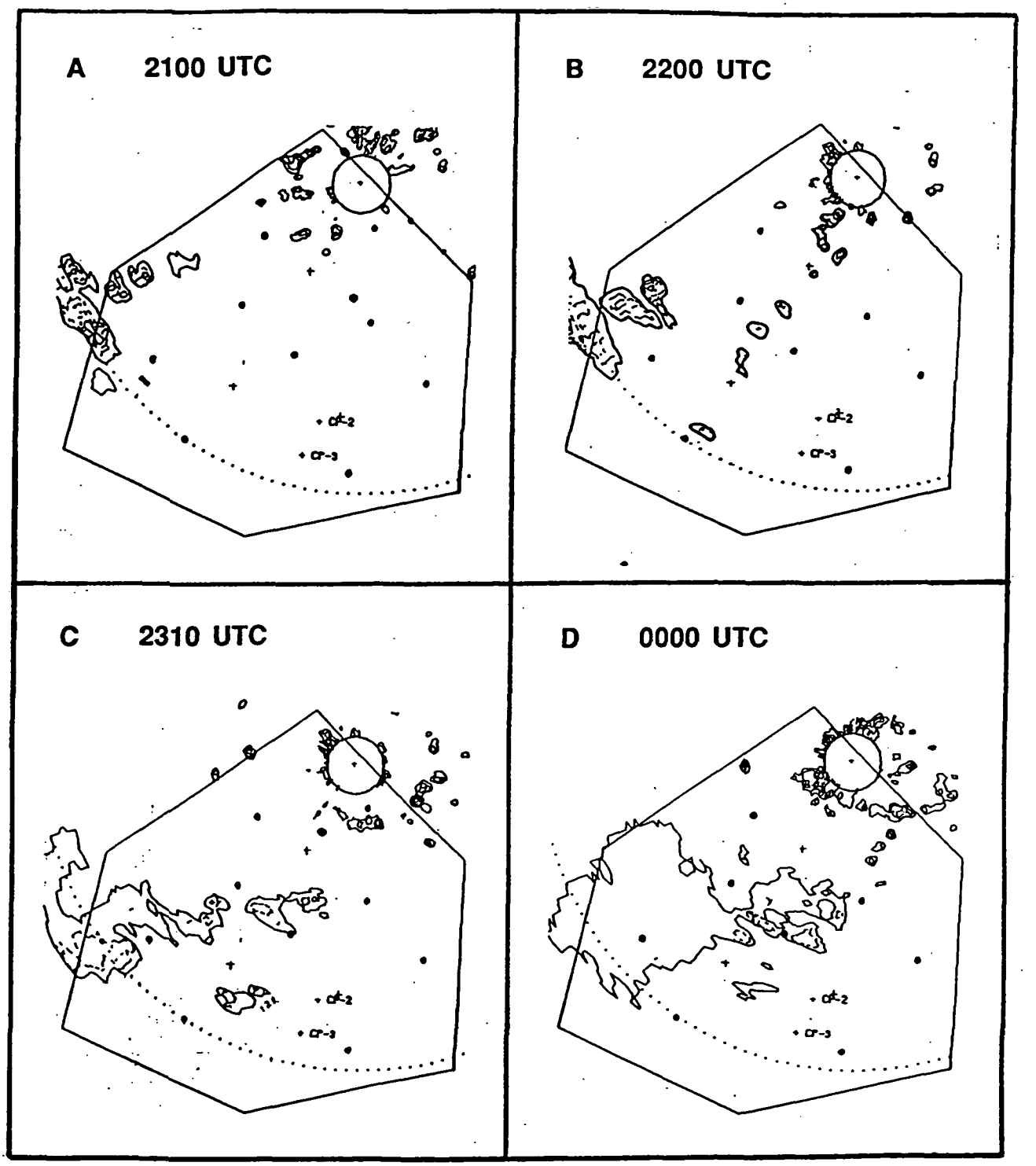

Figure 3 Reflectivities from the Nashville National Weather Service WSR-57 radar at (a) 2100 UTC 28 June, (b) 2200, (c) 2310, and (d) 0000 UTC 29 June. The corners of the hexagon are the outer meso-β COHMEX rawinsonde network stations.

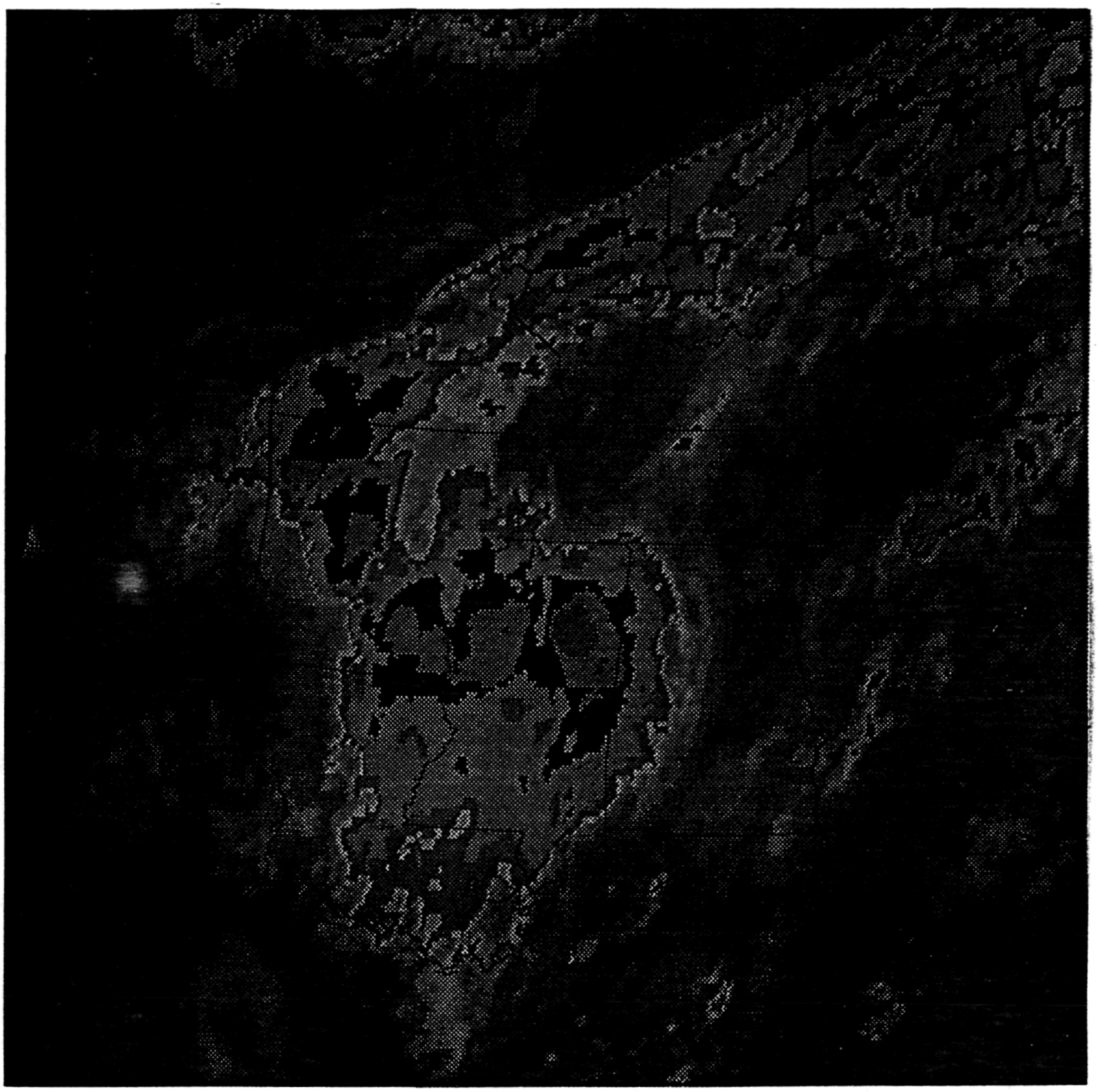

Figure 4 The four sources of synthetic data for the 1200 UTC 28 June moisture assimilation experiment. (a) GOES infrared satellite image, (b) GOES visible satellite image, (c) manually-derived radar VIP levels, and (d) surface-based cloud ceiling height observations (in hundreds of feet).

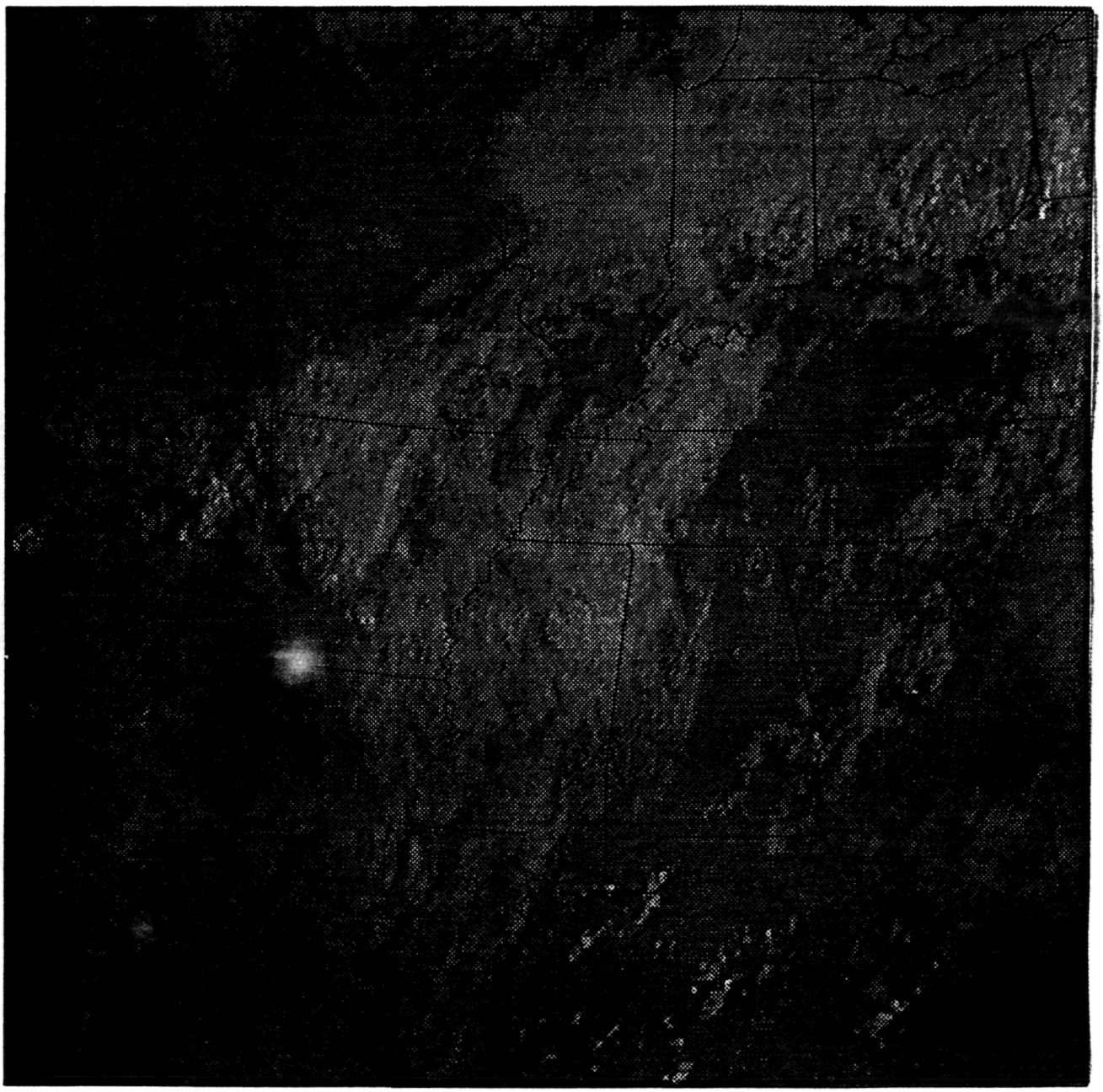

Figure 4 (continued)

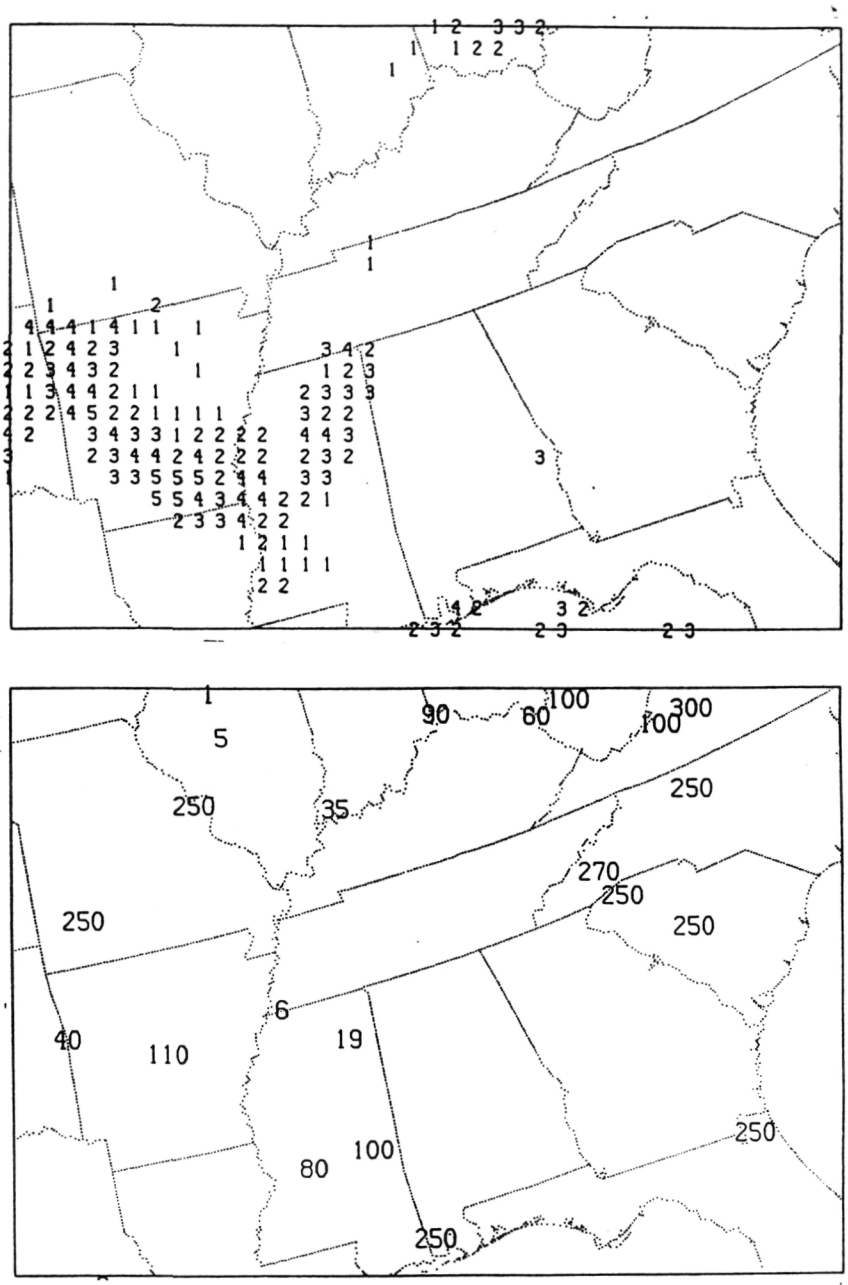

Figure 4 (continued)

Figure 5 (Following two pages) At 1200 UTC 28 June, low level relative humidity field (a) without moisture assimilation, and (b) with the full moisture assimilation scheme.

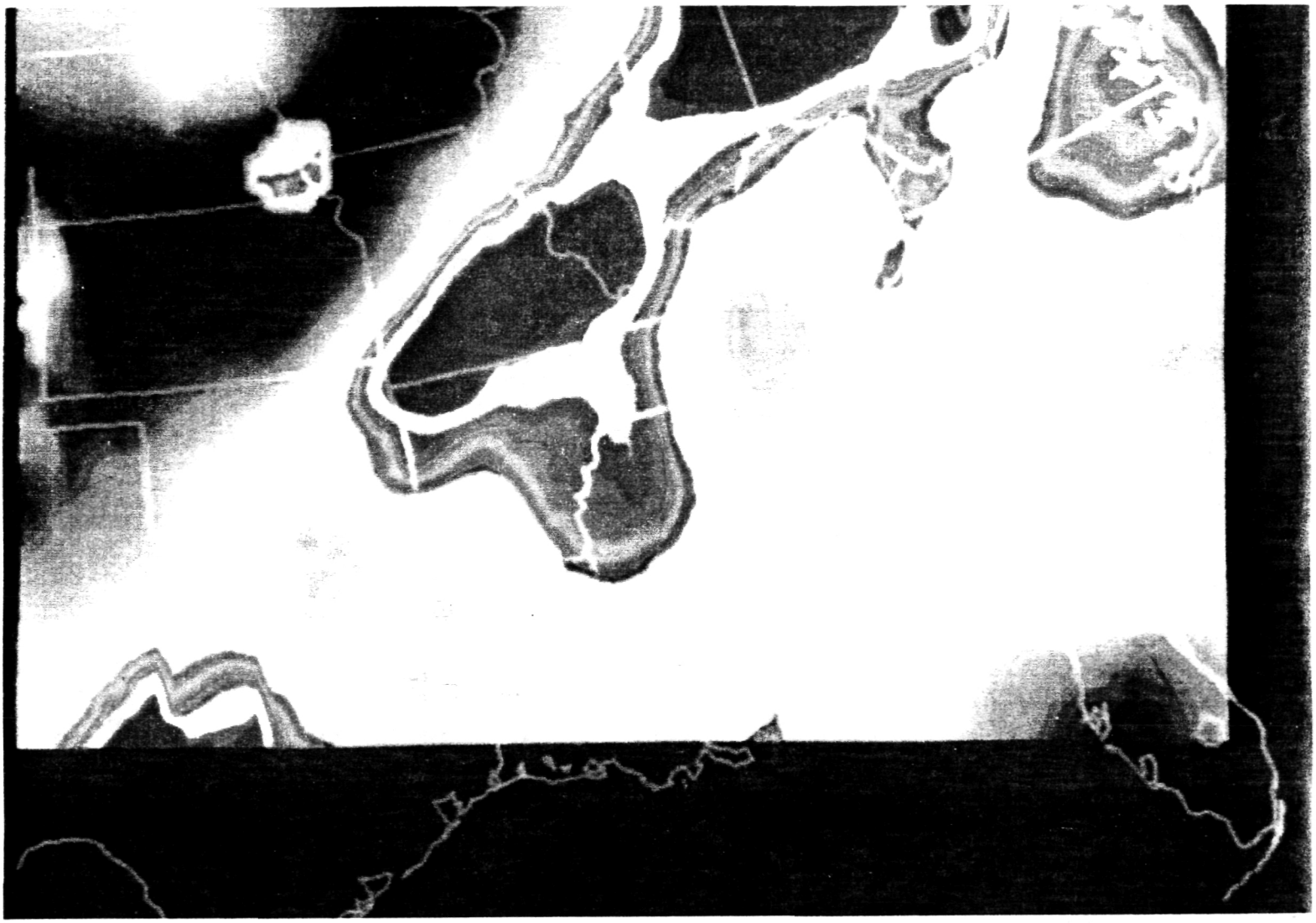

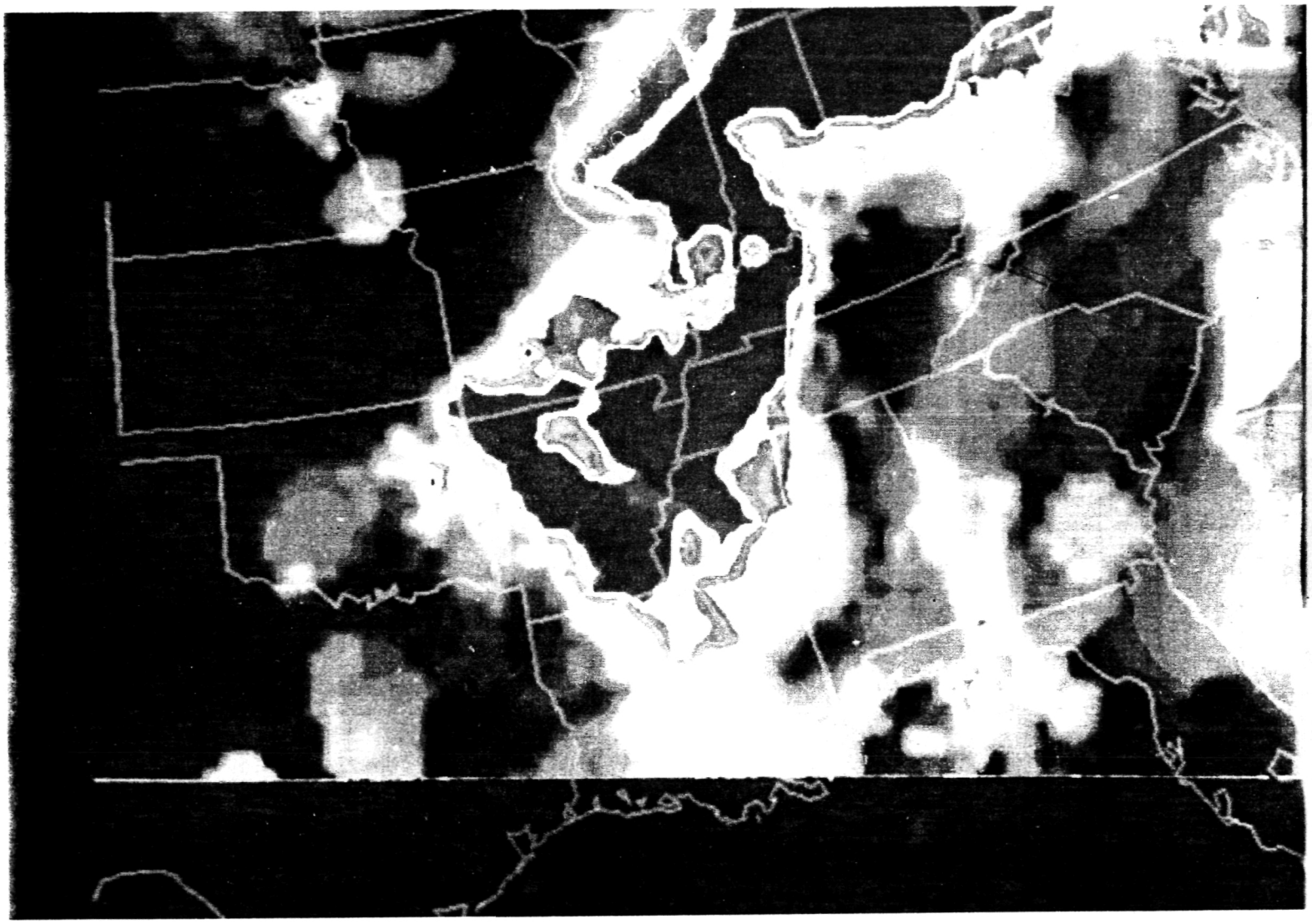

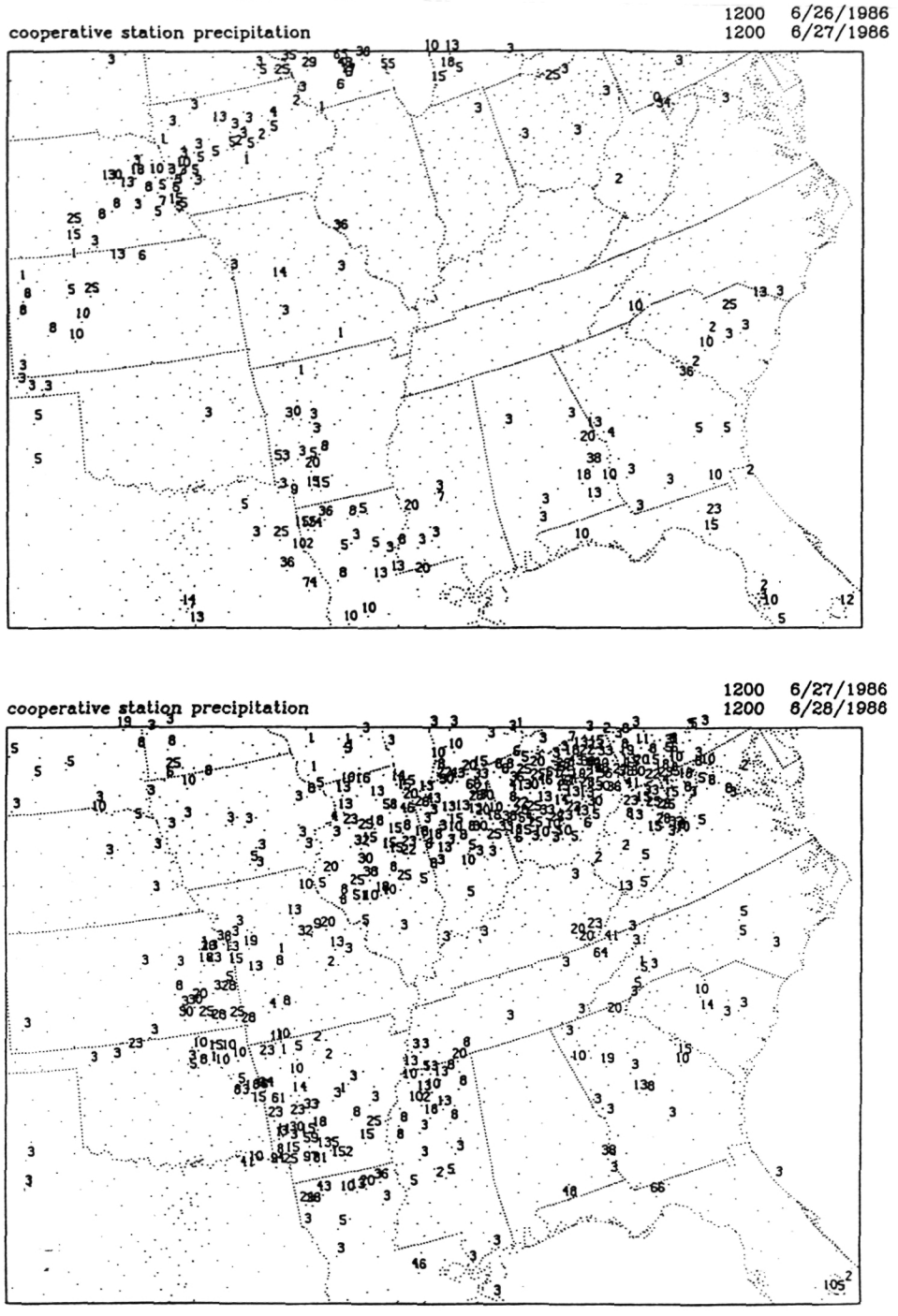

Figure 6 Cooperative observer point observations of rainfall (mm) for twenty four hour periods from (a) 1200 UTC 26 June to 1200 UTC 27 June, and (b) 1200 UTC 27 June to 1200 UTC 28 June. Each point represents a cooperative station (only stations with precipitation reports during the general period are shown).

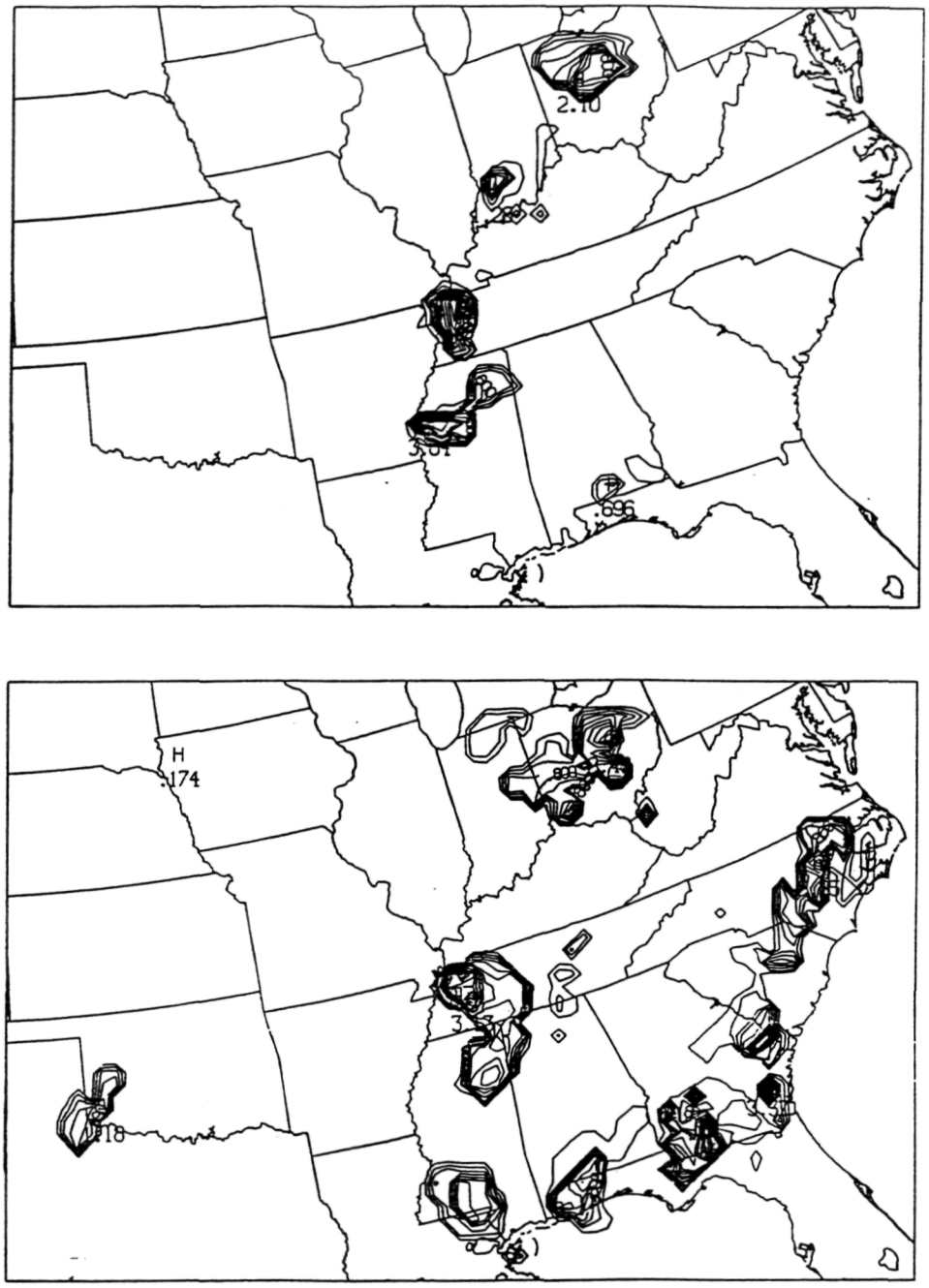

Figure 7 Convective precipitation (mm) for the moisture-enhanced simulation accumulated over the 15 min prior to (a) 1500 UTC 28 June, (b) 1800 UTC, (c) 2100 UTC, and (d) 0000 UTC 29 June. Compare these plots to Figure 2b-e.

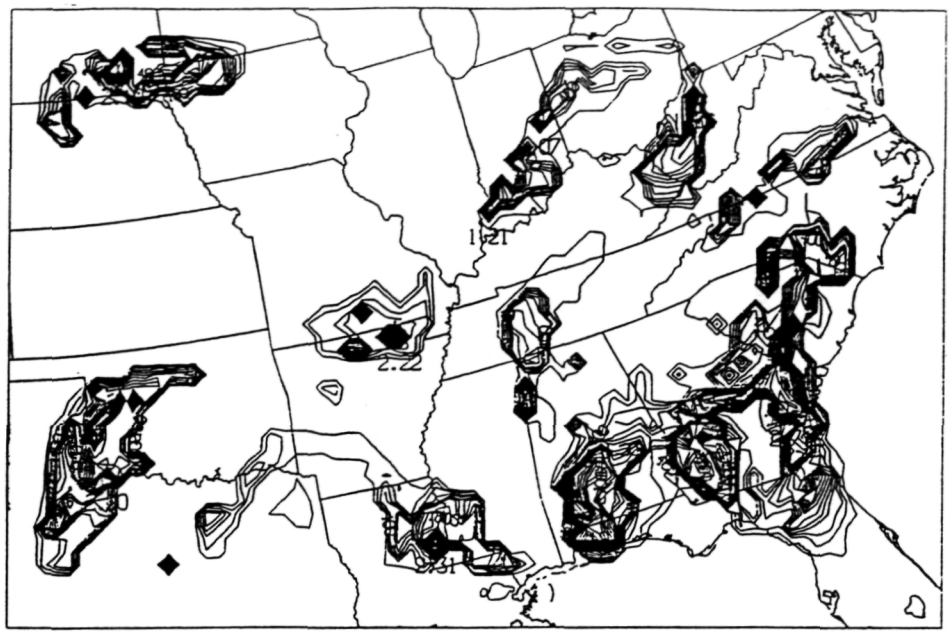

C

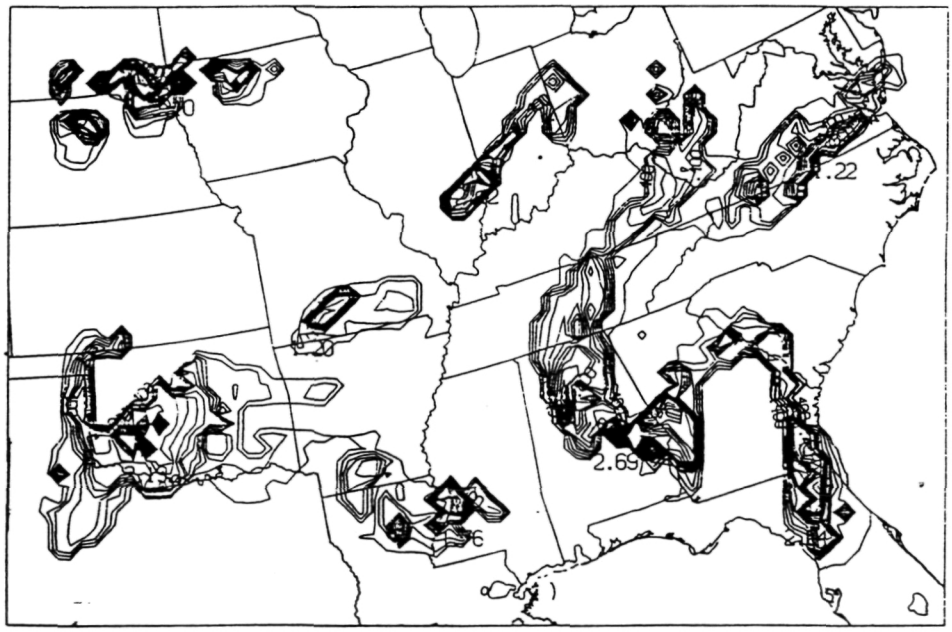

D

Figure 7 (continued)

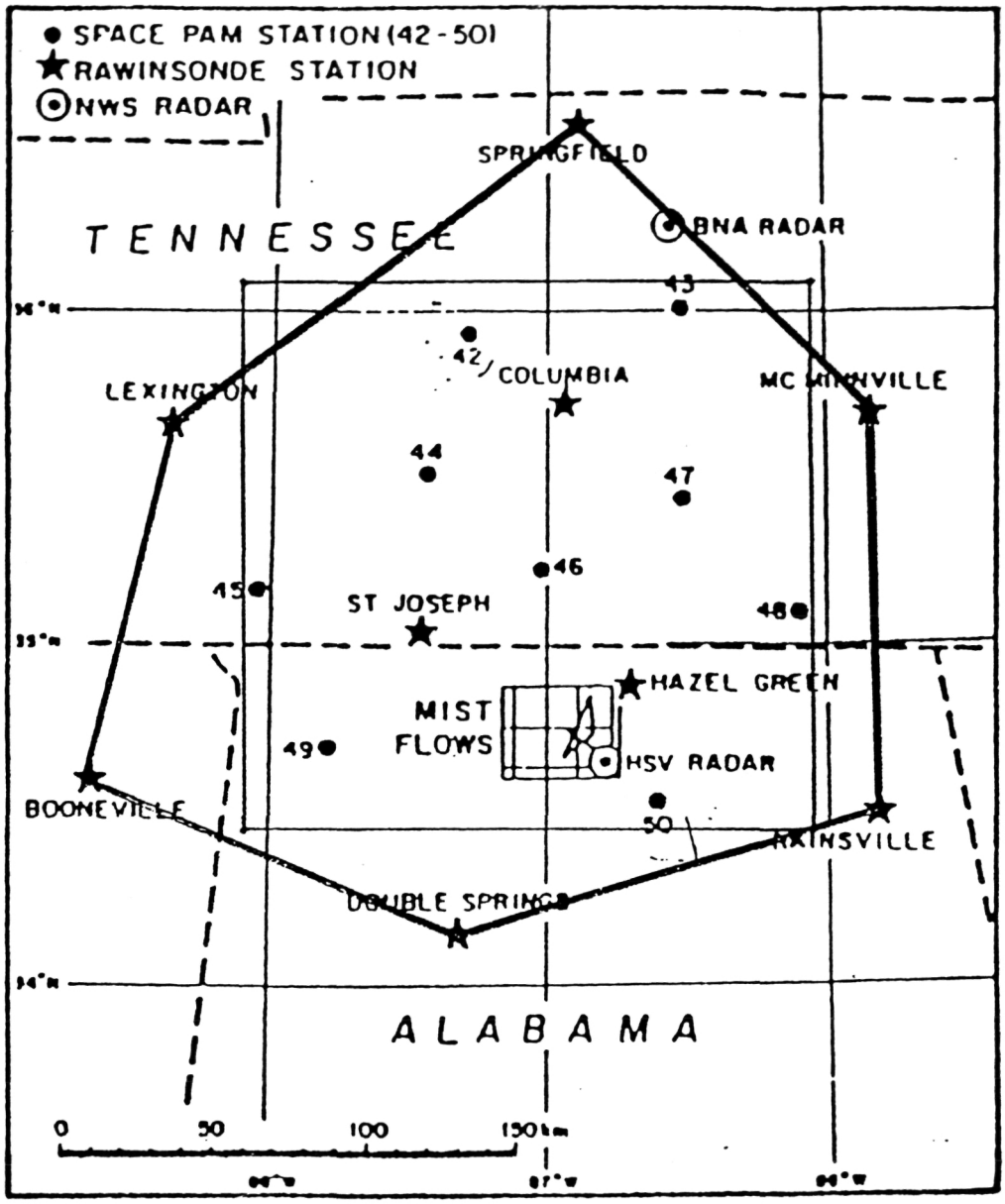

Figure 8 The COHMEX meso-β scale observational network. The rawinsonde stations are denoted by stars, and the surface PAM stations by dots (which are numbered from 42 to 50). The NWS WSR-57 radar is located at Nashville (BNA), TN. The three Doppler radars are all located near Huntsville, AL (HSV). Distance scale is shown at the bottom. The box mostly inside the hexagon is the domain for the TASS 3-D initialization simulation.

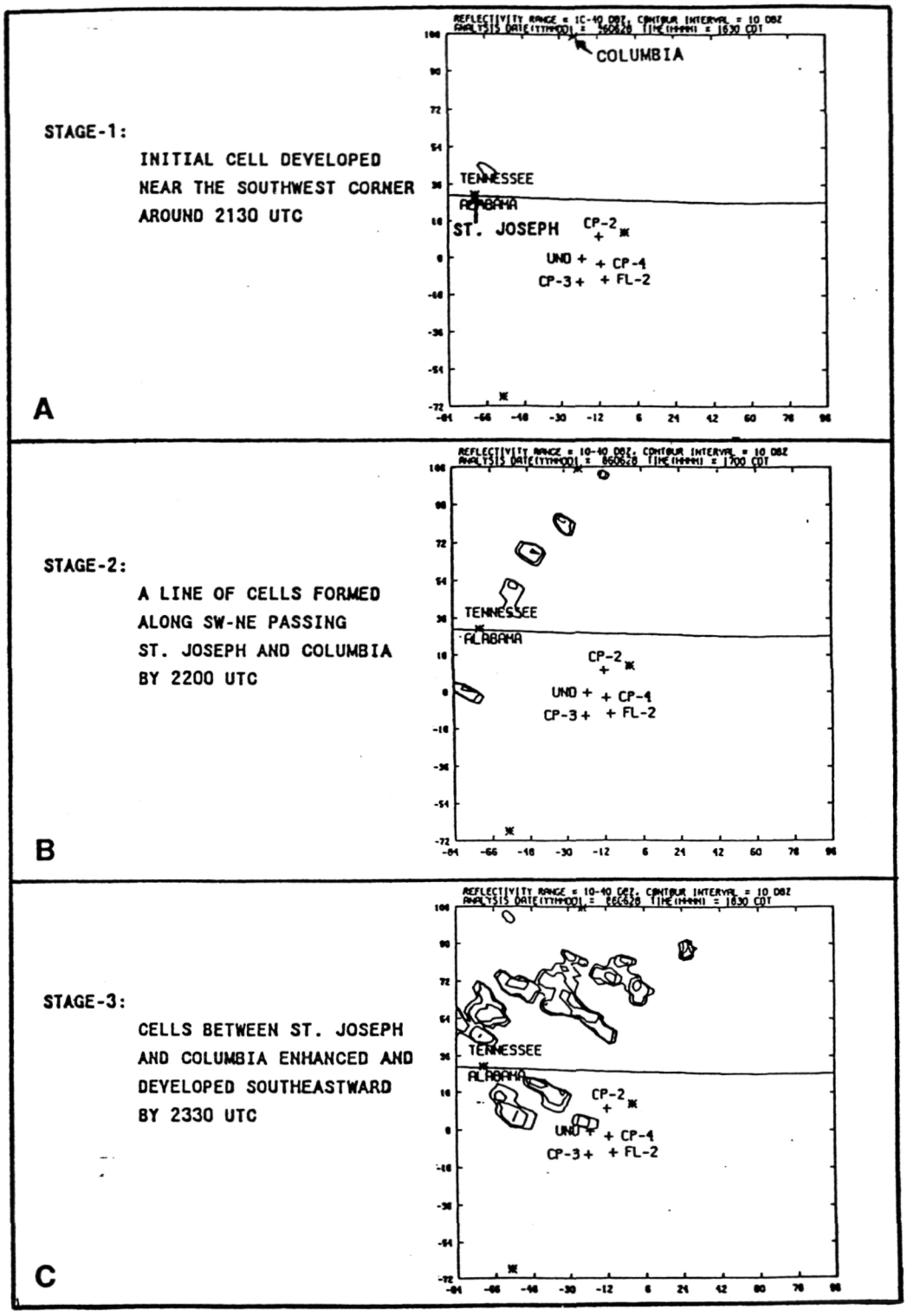

Figure 9 Observed radar reflectivity fields by the CP-4 Doppler radar, which is located (as shown) near Huntsville, AL, looking toward the northwest, at (a) 2130 UTC; (b) 2200 UTC and (c) 2330 UTC.

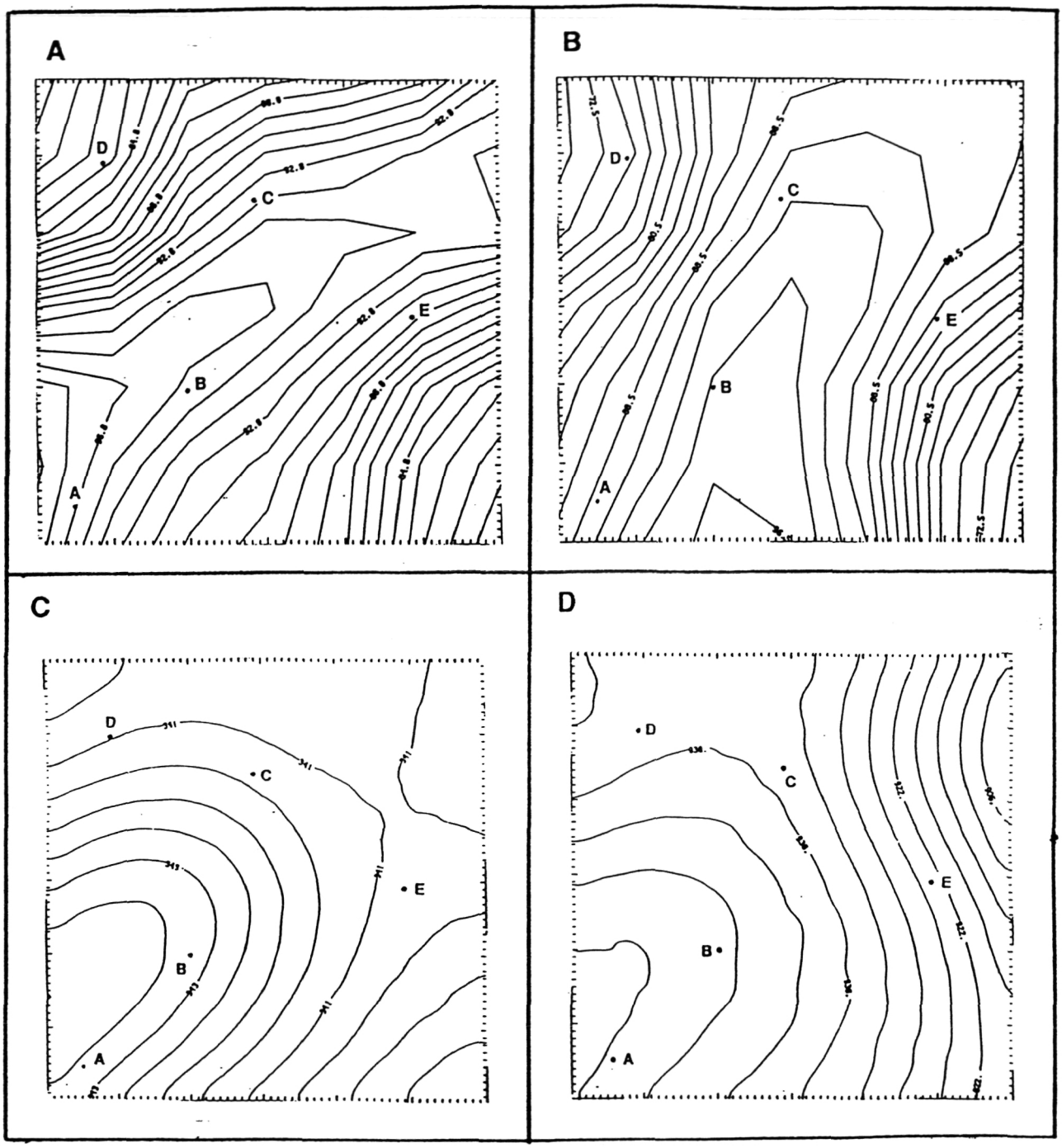

Figure 10 Observed moisture features over the TASS grid domain at 0000 UTC 29 June. Horizontal relative humidity fields at (a) 850 mb and (b) 750 mb. (c) Moist static energy, and (d) lifting condensation level (mb, contoured every 4 mb). The domain covers the box shown in Fig. 8.

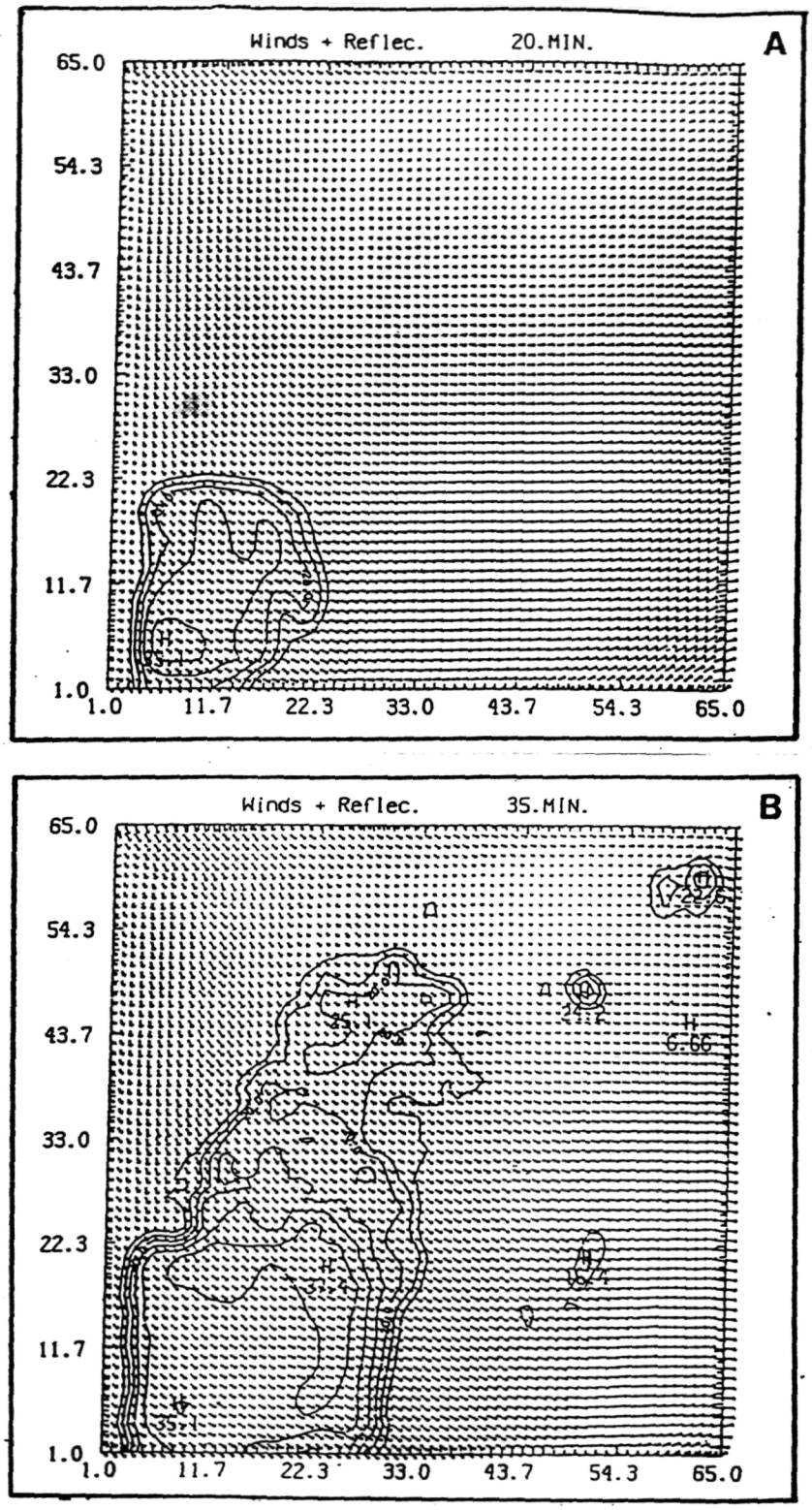

Figure 11 Mass-weighted TASS reflectivities and horizontal wind field within the 1-4 km layer over the model domain at (a) 20 min, (b) 35 min, and (c) 50 min of control simulation. Reflectivities are contoured at 10, 20, 30, 40 dBZ, while the length of one grid of the plotted wind vectors denotes a wind speed of 8 m s^{-1}.

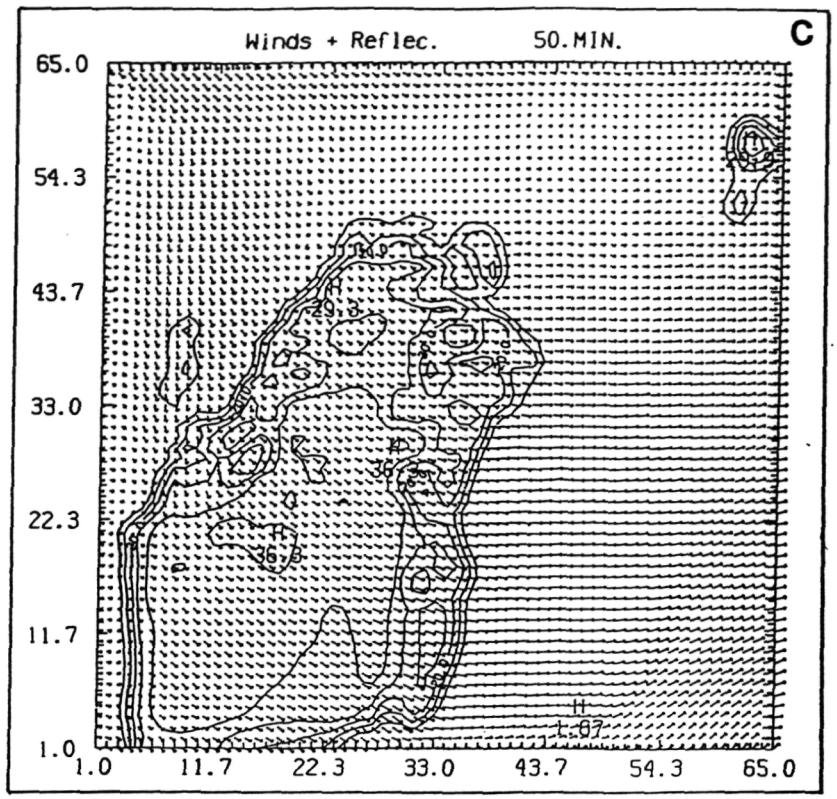

Figure 11 (continued)

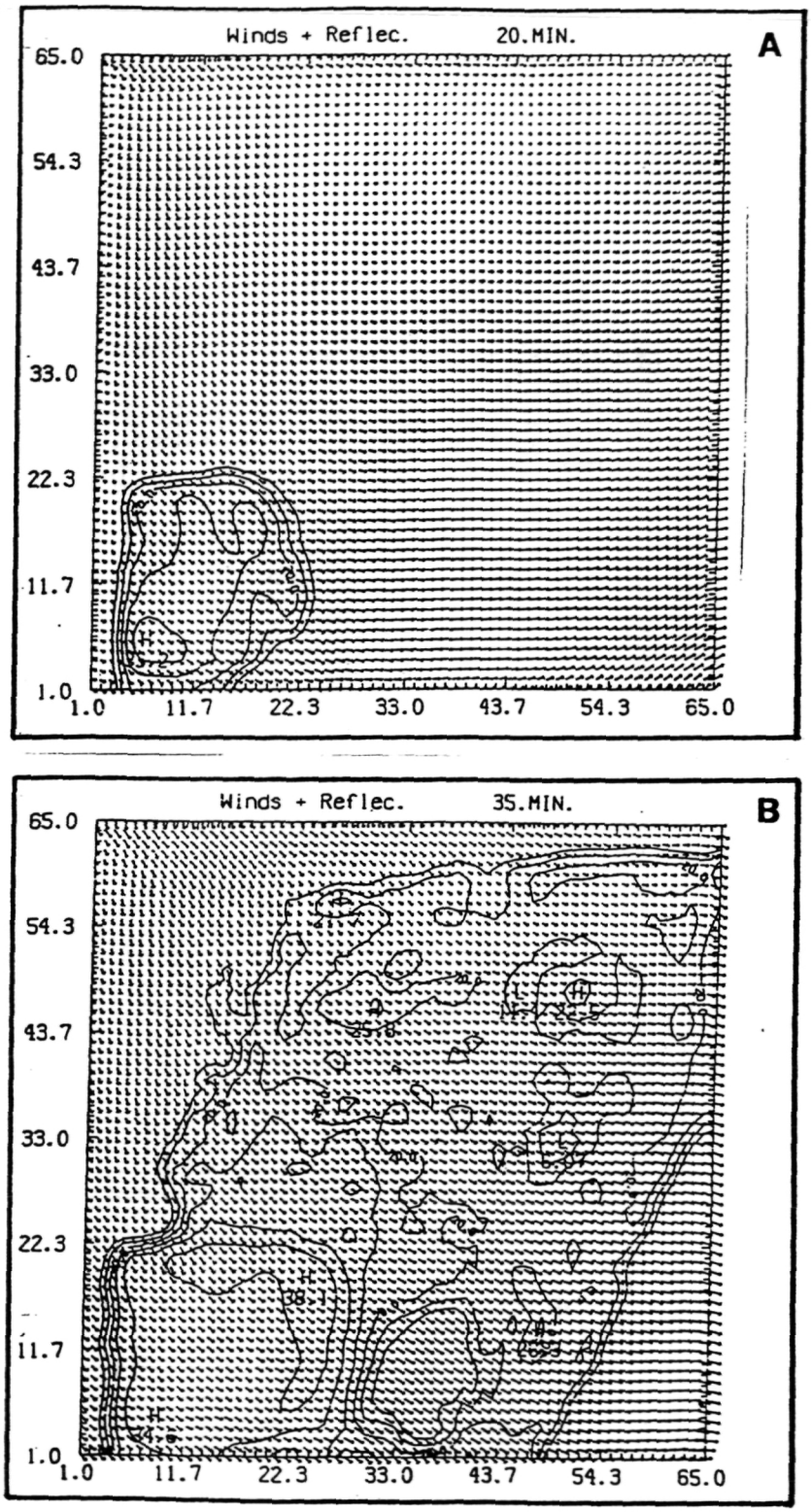

Figure 12 Same as Figure 11 except for the simulation in which the lowest level of input data are replaced by PAM data; the times are (a) 20 min, (b) 35 min, and (c) 50 min.

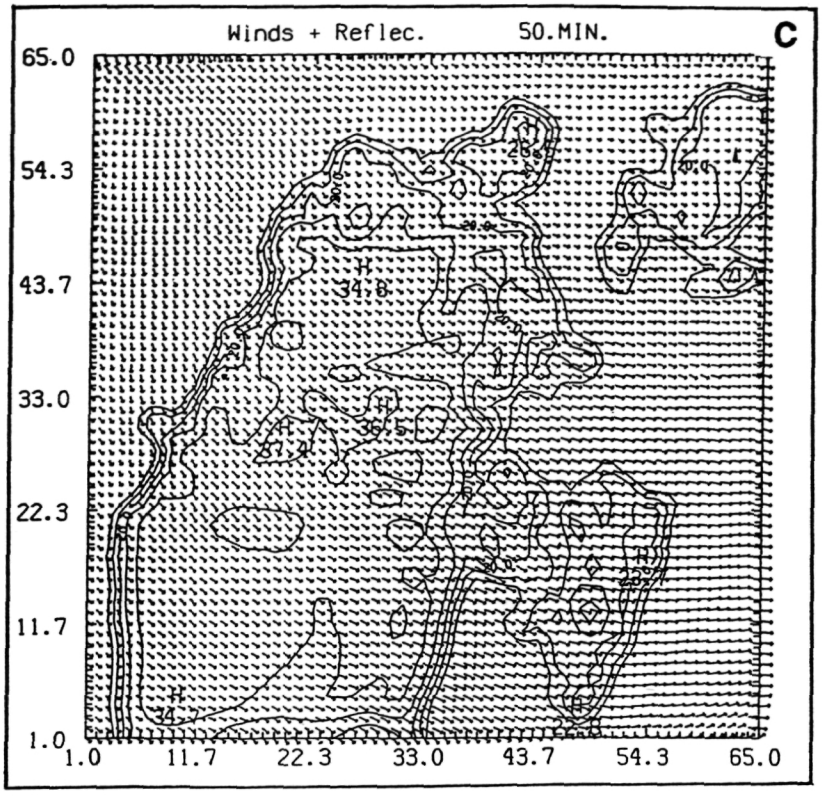

Figure 12 (continued)

Land Use Category	Albedo	Bowen Ratio
11 Residential	.15	.80
12 Commercial and Services	.22	.90
13 Industrial	.20	.88
14 Transportation, Communications, Utilities	.20	.90
15 Industrial and Commercial Complexes	.20	.85
16 Mixed Urban or Built-up Land	.20	.85
17 Other Urban or Built-up Land	.20	.85
21 Cropland and Pasture	.20	.45
22 Orchards, Groves, Vineyards, Nurseries, etc.	.20	.45
23 Confined Feeding Operations	.20	.45
24 Other Agricultural Land	.20	.45
31 Herbaceous Rangeland	.15	.60
32 Shrub and Brush Rangeland	.15	.60
33 Mixed Rangeland	.15	.60
41 Deciduous Forest Land	.15	.30
42 Evergreen Forest Land	.15	.30
43 Mixed Forest Land	.15	.30
51 Streams and Canals	.10	.00
52 Lakes	.10	.00
53 Reservoirs	.10	.00
54 Bays and Estuaries	.10	.00
61 Forested Wetland	.10	.20
62 Nonforested Wetland	.10	.20
71 Dry Salt Flats	.30	.70
72 Beaches	.30	.70
73 Sandy Areas Other than Beaches	.30	.70
74 Bare Exposed Rock	.30	.70
75 Strip Mines, Quarries, Gravel Pits	.30	.70
76 Transitional Areas	.30	.70
77 Mixed Barren Land	.30	.70

Table 1 Land use classifications with estimated surface characteristics.

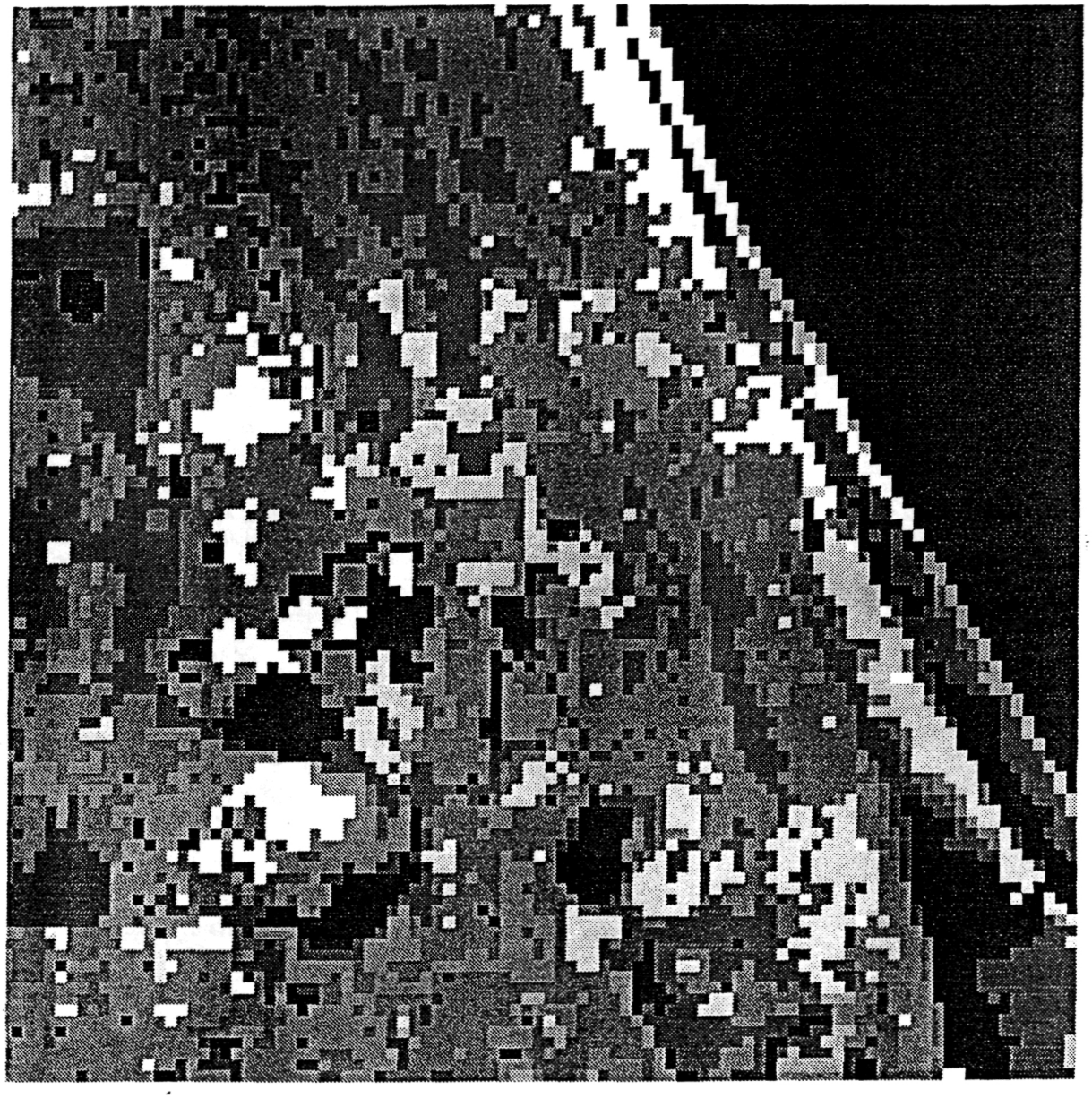

Figure 13 Pattern of sensible heat flux over the TASS model domain derived from land use data. Light areas represent large fluxes. The area covered extends from just north of Orlando, FL on the southwest corner to Daytona Beach, FL on the northeast coastline. The resolution of the image is 750 m.

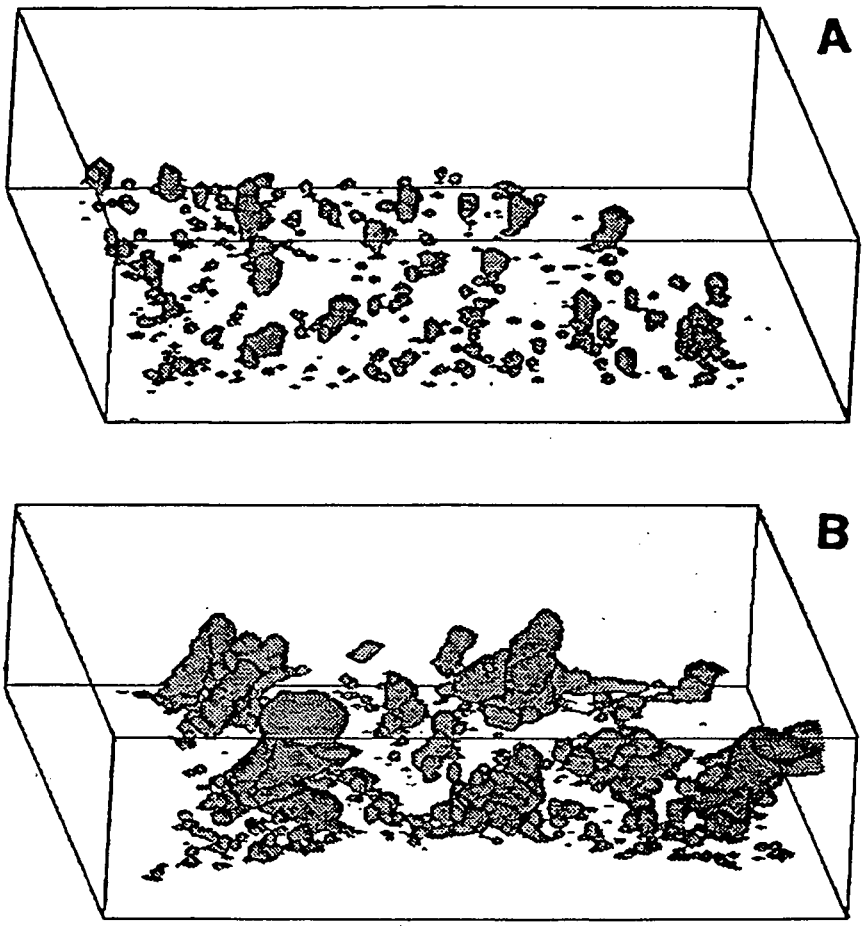

Figure 14 Three-dimensional simulated cloud perspectives (defined by the cloud water and ice fields) after (a) 90 min, and (b) 180 min. The view is from the south looking north. .

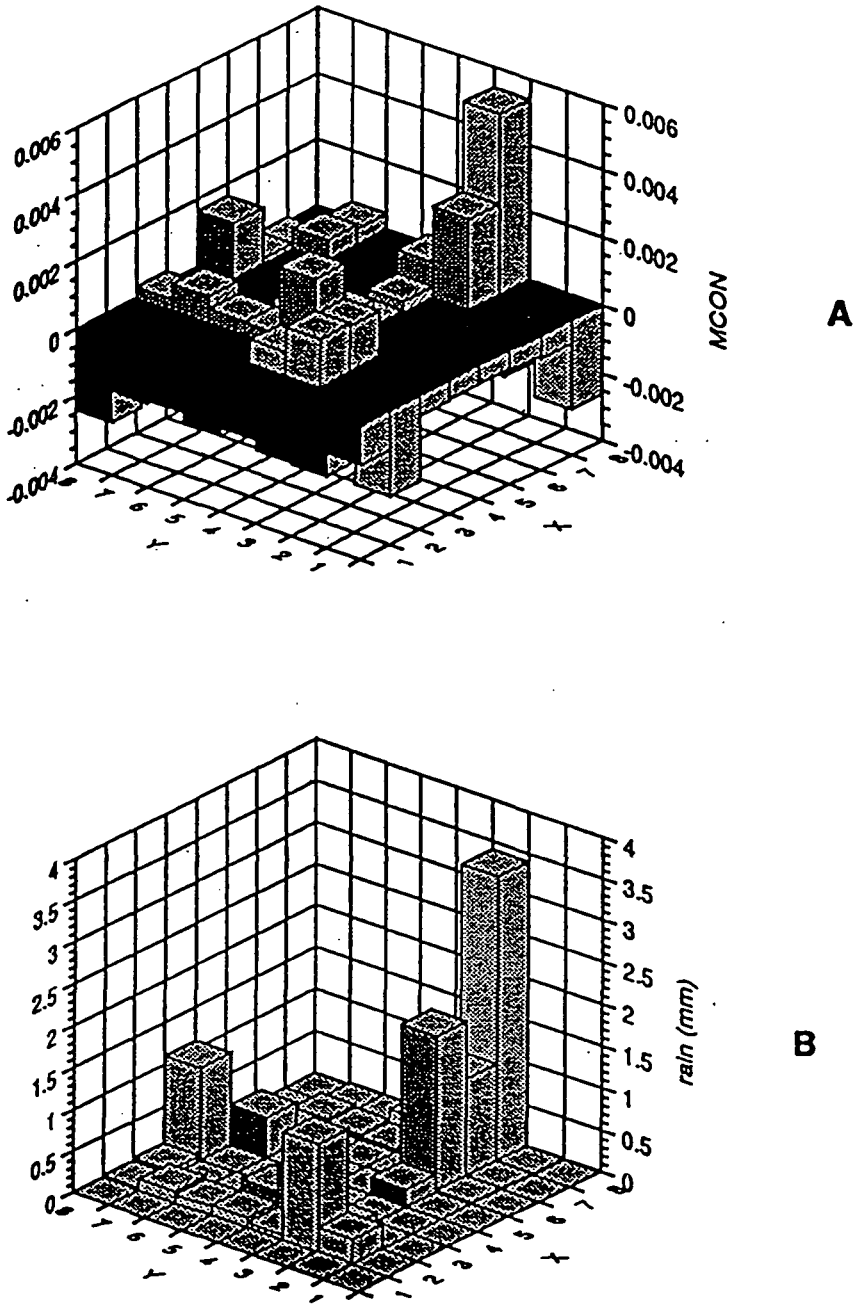

Figure 15 Spatial patterns of (a) moisture convergence and (b) accumulated rainfall in the interval from 90 to 120 min for the 8x8 grid of 8.25 km mesoscale boxes averaged from TASS data. The view is from the southwest.

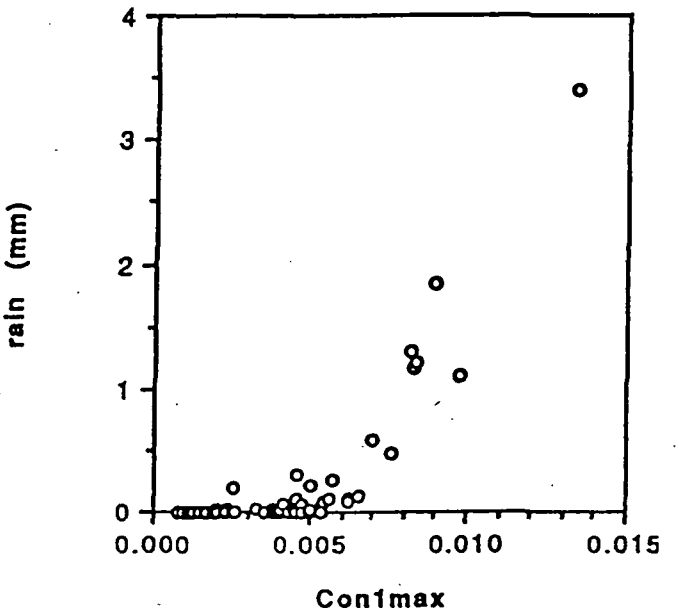

Figure 16 Scatter plot of maximum subgrid convergence in lowest TASS model level versus rainfall from 135 to 165 min of simulation for the 8.25 km boxes

3. Convective Evolution Studies

The general intent of studies concerning the evolution in space and time of modeled convection was to investigate the parameterization problem. First, TASS simulations were carried out for a set of nine soundings derived from COHMEX observations, in order to compare TASS results to observations, and to evaluate the suitability of using TASS results as a replacement for a parameterization scheme. Second, the two schemes included in the MASS model, the Kuo and Fritsch-Chappell schemes, were compared to each other in various ways to evaluate their effectiveness.

3.1 A Tale of Nine Boxes: Divided TASS Simulations

Due to limited physical understanding and computational resources, nonhydrostatic, convectively explicit models are commonly initialized by horizontally homogeneous fields together with a warm thermal "bubble", rather than with a full three-dimensional dataset containing the essential forcing mechanism(s) of deep convection. The following work is designed to study whether such a model can discriminate between the usually subtle thermodynamic variations on meso-β scale (20-200 km), such that by performing a group of such model runs (each initialized with a bubble), the desired mesoscale convective evolution can be produced or at least improved from that produced with the use of a large scale model with a parameterized treatment of cumulus convection.

In this study, the COHMEX 28 June convective event was selected for a set of divided meso-β experiments which were intended to address the convective evolution problem with a conventional nonhydrostatic model approach. The following questions were considered:

(1) Can a meso-β scale convective distribution be produced numerically by performing a group of convectively explicit simulations?
(2) What physical processes (in the model) produce the desired convective distribution, and how?
(3) What are the limitations, and therefore, what other numerical approach must also be incorporated for the purpose of understanding such meso-β scale weather events?

An observational dataset for the June 28 case was constructed from the 0000 UTC 29 June mesonet COHMEX rawinsonde soundings and surface PAM stations. For verification purposes, the observed box-averaged (from PAM station

measurements) precipitation (mm) for the period 2330 UTC 28 June to 0130 UTC 29 June is shown in Fig. 17a. Very little precipitation falls over this region during the few hours after 0130 UTC. During this period, the strongest convection moves eastward from box 4 to box 5, with box 5 recording the heaviest precipitation. This case was described in more detail in Sections 2.1 and 2.3.

A Barnes objective analysis scheme was used to produce a dataset of temperature, wind components and moisture on a 50 km grid which encompassed the entire COHMEX meso-β rawinsonde array. The analysis grid covered the entire entire meso-β scale rawinsonde network as shown in each panel of Fig. 17. The data from the 50 km analysis grid was then interpolated with a cubic spline interpolation scheme to a 1 km grid over the area covered by the nine boxes depicted in Fig. 17. Each one of the nine boxes enclosed an array of 64 x 64 of these 1 km grid points. Three hour TASS simulations with 20 vertical levels were then run for each of these 64 x 64 arrays.

The first set of TASS simulations used horizontally uniform initial conditions in which the cloud was initiated by adding a buoyant bubble to the initial state. The vertical profiles of model variables for each box were obtained by averaging each variable at each level over the 64 x 64 array. The results shown in Fig. 17b indicate that the general pattern of precipitation was acceptable, but that the amounts are much too large in the convectively active boxes. A second set of TASS simulation results are shown in Fig. 17c. These simulations were initialized in a manner identical to those shown in Fig. 17b but used a modified set of lateral boundary conditions. In this formulation the dependent variables were specified at the inflow boundary points and were computed from a radiation condition at the outflow boundary points. This formulation is in contrast to the mass conservation boundary conditions used for the Fig. 17b simulations. Fig. 17c indicates that the effect of the modified boundary conditions is to significantly reduce the amount of precipitation produced in all of the boxes. However, the amount of precipitation is still too high in boxes 4 and 1 relative to box 5. Results from a third set of simulations is shown in Fig. 17d. This set of simulations used the same boundary conditions as those shown in Fig. 17c. However, the initial state was taken directly from the interpolated 1 km dataset without horizontal averaging. Thus, horizontal gradients of temperature, moisture and wind were present in the initial state. No bubble was used to initiate convection. The results in Fig. 17d indicate that this set of simulations produces the most reasonable precipitation magnitudes in each of the boxes. However, the maximum precipitation occurs in box 4 rather than as observed in box 5. This is probably due to the fact that no time dependent boundary information is incorporated into the model integration in any of the boxes. As a result, the progression of the convective system from box 4 eastward into box 5 as

observed in nature cannot occur in the divided simulations.

The above simulations clearly indicate that even with the use of exactly the same initial bubble, the model seems to be able to distinguish among soundings which do not show dramatic differences. There must be, therefore, certain processes created, perhaps non-linearly, in the model during the simulation such that the model is able to "decide" where and how deep convection should be produced, while in other situations producing only shallow or no convection. While a precipitation distribution resembling the observed distribution was produced by the best sets of simulations, the results were very sensitive to the lateral boundary conditions, which is to be expected for such small domains.

One of the purposes of these experiments was to show that the TASS model could theoretically be used as a sort of glorified parameterization scheme, producing useful information from simple horizontally homogeneous initial conditions initiated with a warm bubble (very similar to the assumptions used in the one-dimensional cloud models used in convective parameterization schemes). However, the fact that the best set of simulations used three-dimensional initial conditions without a bubble points the way to the more sophisticated nonhydrostatic simulation presented in Section 2.3.

3.2 *The Battle of the Schemes: Kuo vs. Fritsch-Chappell*

It is generally accepted that some sort of parameterization of convective processes is necessary for hydrostatic atmospheric models, since they are incapable of resolving the fundamental convective circulations, updrafts on the scale of about 1 km. Models at the lower end of the meso-β scale (10 km) can resolve part of larger storm scale circulations, but important subgrid scale processes still need to be represented by a parameterization scheme (Zhang *et al.*, 1988).

Two widely-used cumulus parameterization schemes are included as a part of the MASS model. The first was developed by Kuo (1965, 1974) and further refined by Anthes (1977a); it will be referred to as the Kuo scheme. This scheme was intended for use in relatively large scale models, with grid spacings generally larger than 50 km. The fundamental closure assumption made by the Kuo scheme is that the convective precipitation rate is instantaneously related to the total column moisture convergence, given by

$$Moisture\,Convergence = -\frac{1}{g}\int_0^{p_s} \nabla \cdot Vq \, dp \,, \tag{3.1}$$

where g is the acceleration due to gravity, V is the horizontal velocity vector, q is water vapor mixing ratio, and the integral is taken over the depth of the column by

pressure. The condensational heating represented by a fraction of this moisture convergence (the rest is stored in the column) is then distributed in the vertical by a one-dimensional cloud model. For convection to occur in the Kuo scheme, moisture convergence above a threshold amount must occur, and the atmosphere must be unstable enough to build a deep cloud.

Fritsch and Chappell (1980) presented a scheme intended for use in meso-β scale models with a grid spacing of about 25 km. In addition to the significantly different initiation criteria of the two schemes discussed in Section 2, the closure assumptions also differ substantially. In the Fritsch-Chappell formulation, a time scale is assigned based on the mean wind speed at each model grid point. Then, a convective intensity is assumed which will reduce the initial Available Buoyant Energy (ABE) by a given fractional amount during the course of one convective time period. The one-dimensional cloud model is more sophisticated than for the Kuo scheme; it includes a formulation for cool downdrafts as well as vertical momentum transfer. ABE removal takes place as low level air is progressively replaced by cool downdraft air originated from midlevels, thereby stabilizing the entire column.

In the course of this research effort, both schemes have been used and investigated extensively. In the following paragraphs, results will be presented and discussed, first for the Fritsch-Chappell and then for the Kuo scheme.

A significant part of the original research objectives for this project involved the comparison of one-dimensional cumulus parameterization schemes to TASS results, for the main purpose of evaluating the 1-D schemes. Section 3.1 discussed the TASS divided simulations, in which the TASS model functioned conceptually in the role of a parameterization scheme. In conjunction with that work, the Fritsch-Chappell scheme was tested on the same nine-box sets of COHMEX soundings. A direct comparison of heating and moistening rates between the cloud model and a 1-D scheme is difficult to make, because a parameterization scheme attempts to depict only the subgrid part of the entire convective process, leaving a portion to be explicitly simulated by the mesoscale model. A cloud model simulation, on the other hand, purports to represent the entire convective process explicitly, so that the "convective terms" of the thermodynamic and moisture equations are intertwined with the other terms (*e.g.* advection) in a complex way. Rather than comparing temperature or moisture tendencies, TASS precipitation amounts can be reasonably compared to Fritsch-Chappell convective precipitation fields. Fig. 17 shows the actual and TASS produced precipitation amounts for the nine boxes. Fig. 18 shows results from a series of simple Fritsch-Chappell experiments, in which the scheme was used in a purely 1-D fashion, separate from the MASS model. The results were generally poor; the precipitation patterns

produced did not compare well with either observations or TASS results. Several things either limit the usefulness of the general approach , or were a likely source of problems for these particular experiments:

(1) Close examination of the Fritsch-Chappell results revealed some coding problems which caused strange heating profiles for certain input soundings. The general problem was that the scheme sometimes could not create a downdraft, which made it difficult to remove ABE. Subsequently, unreasonably large upper level heating rates were produced along with large precipitation rates. A much newer version of the scheme was obtained from Dr. J. Michael Fritsch and Dr. Da-Lin Zhang which improved but did not completely eliminate the problem.

(2) The Fritsch-Chappell scheme is quite sensitive to the background vertical velocity, because of the temperature perturbation term which is calculated from the grid scale vertical velocity at the LCL. The vertical velocities inferred from COHMEX rawinsonde data are somewhat suspect since the mesoscale vertical velocities can be expected to significantly vary spatially and temporally in the absence of a strong large scale forcing mechanism.

(3) Practical problems come up when trying to compare results from a scheme at one point in time with results from a complete cloud model simulation covering a period of more than one hour. In the Fig. 18 results, 30 minute (one parameterized convective period) rainfall was simply extrapolated to two hours, ignoring the time-dependent nature of both the background forcing and the (missing) interaction of the scheme with mesoscale model.

A minor effort was made to examine the underlying assumptions of the Fritsch-Chappell scheme through analysis of TASS results. Fig. 19 shows the evolution of Convective Available Potential Energy (CAPE) with time for a simple TASS bubble-initiated run. CAPE removal for boxes of various sizes centered on the initial convection shows the scale dependence of the stabilization process. The smallest scales are stabilized first, followed by larger scales as thunderstorm outflow gradually replaces warm moist low level air with cooler downdraft air. The basic Fritsch-Chappell premise of CAPE (equivalent to ABE) removal as a fundamental process is supported, although in the first 60 minutes (the longest allowed Fritsch-Chappell convective time period), only about one-third of the CAPE is removed. The percentage of removal is considered flexible for the scheme, although the original paper assumed 100% removal.

Both schemes were tested thoroughly in mesoscale simulations. The 28-29 June MASS simulations consisted of two parts: a 75 km coarse mesh simulation beginning at 0000 UTC 28 June, and a 37.5 km nested simulation which used coarse mesh fields a a first guess field for a new preprocessor initialization using 1200 UTC data. A large series of runs were made over the course of the project with various combinations of input data and model physics. Neither the Kuo scheme nor the Fritsch-Chappell scheme produced good results for the 75 km coarse mesh runs, probably reflecting the fact that convective forcing mechanisms (*i.e.* mesoscale low level convergence) are not well-resolved at that scale. Since the Kuo scheme was intended for larger scale models, it was generally used for the coarse mesh simulations. When new data was added to the 37.5 km fine mesh at 1200 UTC, including the moisture assimilation procedure described in Section 2.2, the Fritsch-Chappell scheme produced substantially better results than the Kuo scheme. Fig. 20 shows comparative results from one set of simulations performed fairly early in the project. The precipitation patterns are dramatically different after twelve hours of simulation, despite identical initial conditions. Several factors may explain the superiority of the Fritsch-Chappell meso-β convective forecasts for this case:

(1) The 37.5 km grid spacing (at the standard latitude of 60 °N latitude; the oblique stereographic grid spacing is actually about 30 km in the COHMEX area) is about the grid size for which the Fritsch-Chappell scheme was intended, while the Kuo scheme has generally been used for meso-α or larger scale models.

(2) The Kuo scheme moisture convergence threshold used was 1×10^{-5} kg m^{-2} s^{-1}, the same used by Anthes (1977b) in hurricane simulations. It may be that this threshold is too high for the June 28 weakly forced type of case, resulting in significant mesoscale convergence areas being ignored.

(3) The Anthes (1977a) criteria for the existence of convection are more restrictive than for the Fritsch-Chappell scheme. In the Fritsch-Chappell scheme, convergence is not a *necessary* condition; convection can occur without convergence if the atmosphere is unstable enough, or with only slight convergence. The scheme is also quite sensitive to small amounts of mesoscale lifting through the temperature perturbation term:

$$\Delta T = c_1 \, w_{LCL}^{1/3}, \qquad (3.2)$$

where w_{LCL} is the grid resolved vertical velocity (in cm s^{-1}) and c_1 is a dimensional constant with a value of one, so that 1 cm s^{-1} of grid-resolved lifting results in a 1°C positive temperature perturbation. The temperature difference ΔT is then added to the updraft at the LCL in the determination of parcel buoyancy. The Fritsch-Chappell scheme then, may be more appropriate for cases with weak large scale forcing, such as the June 28 COHMEX case.

(4) The Fritsch-Chappell scheme contains a parameterization for convective downdrafts formed from evaporative cooling, while the Kuo scheme does not. Meso-β thunderstorm outflow boundaries can initiate secondary convection, which may be important for this case.

The Fritsch-Chappell scheme was intended to be used only over a very narrow range of mesoscale model grid spacings (about 25 km), because assumptions are made which are strongly scale dependent. This research supports the notion that the scheme is not applicable outside of that range. Analysis of cloud model results for the Florida simulation discussed in Section 2.4 compared parts of the two parameterization schemes. The Fritsch-Chappell scheme was applied to the 8.25 km mesoscale boxes, where data for each box was averaged from the TASS 750 m grid. Fig. 21 shows that while the Fritsch-Chappell scheme greatly overpredicted the coverage of convection, a simple moisture convergence criterion successfully predicted the general pattern of convection. Since the Kuo scheme has been considered to be well-suited only for large scale models, it is interesting that the moisture convergence criterion performs so well on an 8.25 km grid. This suggests that when the relevant convergence is well resolved by the model grid (as in the Florida TASS-derived dataset), the Kuo-type of closure assumption has validity, even at relatively small grid spacings of about 10 km.

To reinforce the point, a series of 10.5 km resolution MASS simulations were carried out using initial conditions and surface heating and moistening functions which were as similar as possible to the TASS Florida simulation described earlier. A simulation using the Fritsch-Chappell parameterization produced unrealistic convection, while the Kuo scheme produced very reasonable results (Fig. 22 and Fig. 23). The Fritsch-Chappell scheme allowed convection to begin over almost the entire domain simultaneously (Fig. 23) and produced downdrafts which were far too strong; they replaced all of the low level air in the model domain after a few hours, suggesting again that the scheme is not appropriate for models with resolutions below about 15 or 20 km.

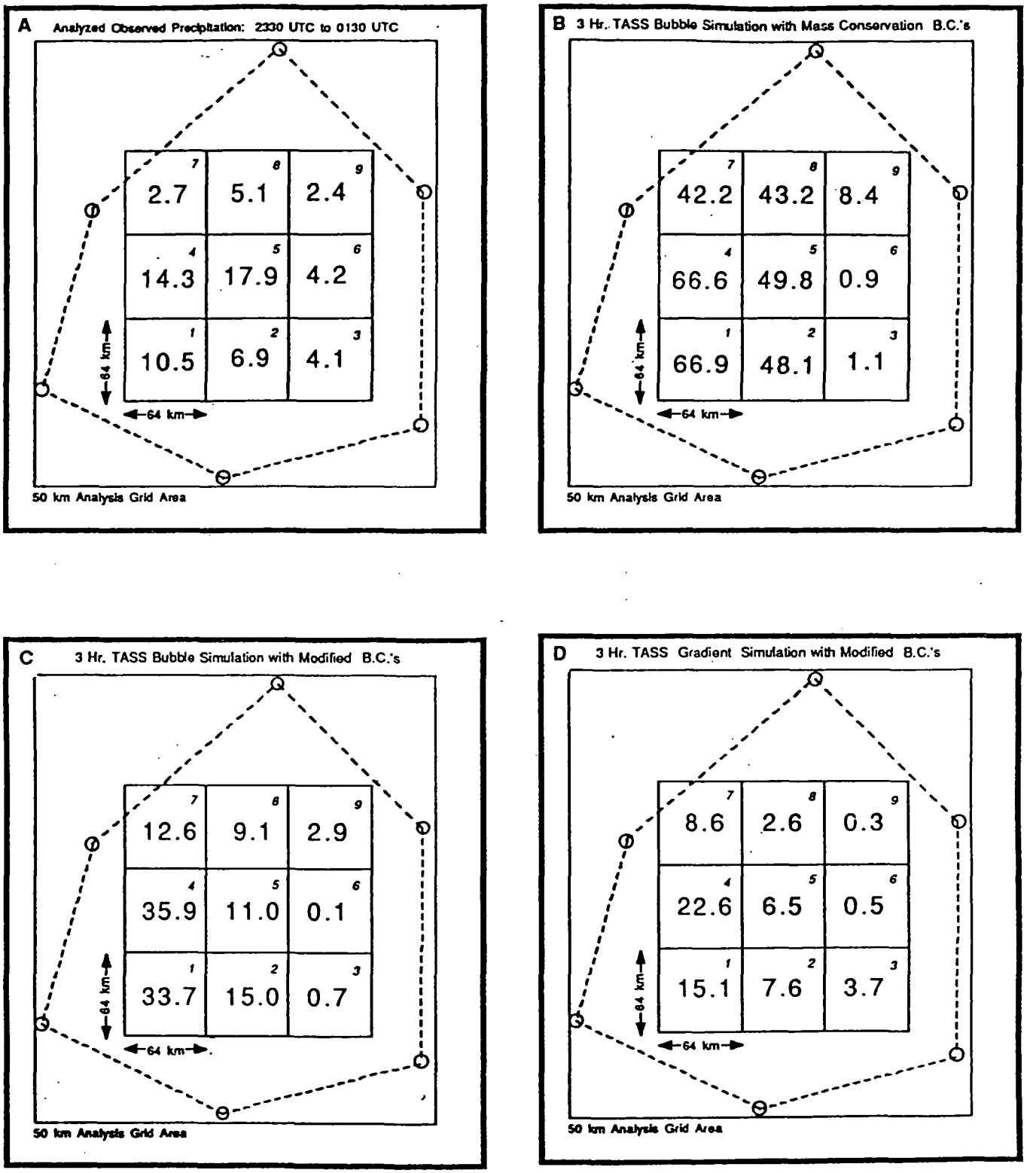

Figure 17 Comparison of observed and TASS model generated precipitation for the June 28 COHMEX case. The large numerals in the numbered boxes represent box-averaged precipitation amounts in mm. The circles depict the location of the outer ring of meso-β scale COHMEX rawinsonde sites.

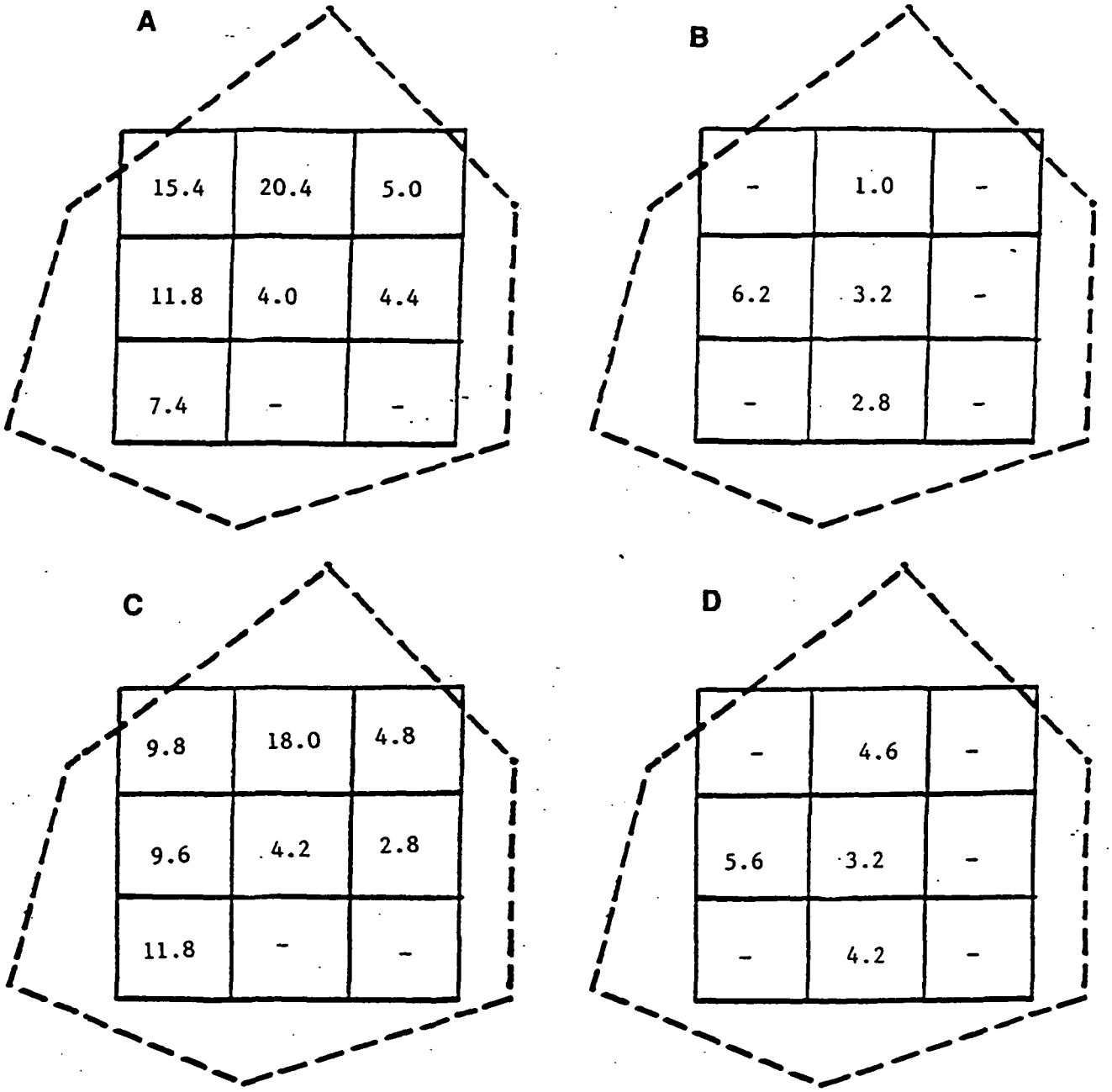

Figure 18 Precipitation amounts (extrapolated to two hours) from a one-dimensional version of the Fritsch-Chappell cumulus parameterization scheme. (a) and (c) used soundings derived from 2100 UTC 28 June data, while (b) and (d) used 0000 UTC 29 June soundings. (a) and (b) assumed no background vertical velocity, while (c) and (d) used vertical velocity profiles inferred from kinematic calculations from meso-β rawinsonde data.

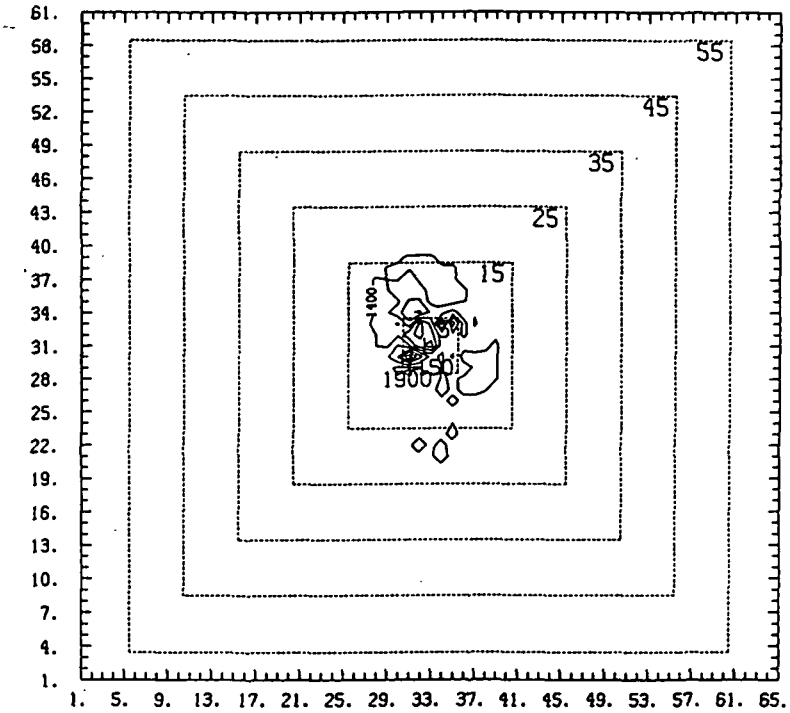

A

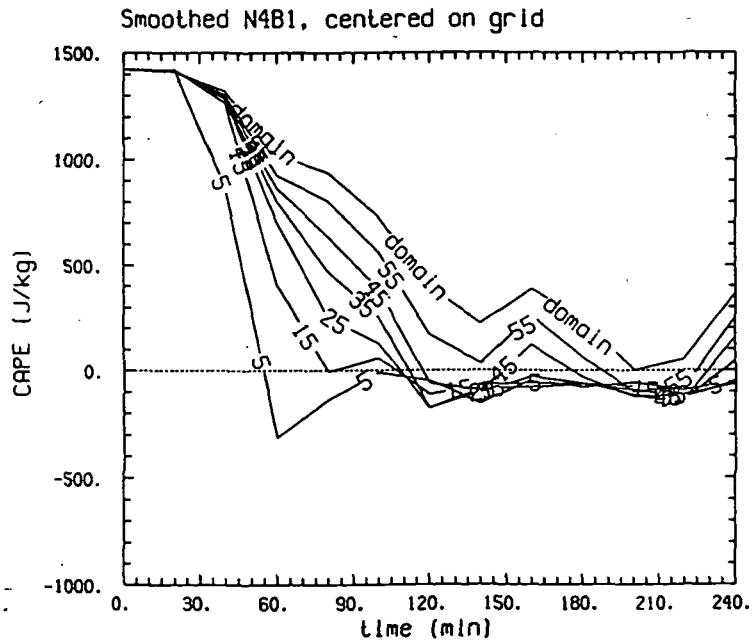

B

Figure 19 (a) TASS 65x61 grid near the beginning of a bubble-initiated convective simulation. The modeled CAPE field is shown near the beginning of the simulation; except for the area in the middle where convection is beginning, the CAPE is about 1400 $m^2 s^{-2}$ everywhere. The dashed boxes show the areas over which CAPE is averaged. (b) Time evolution of CAPE for the boxes shown in (a).

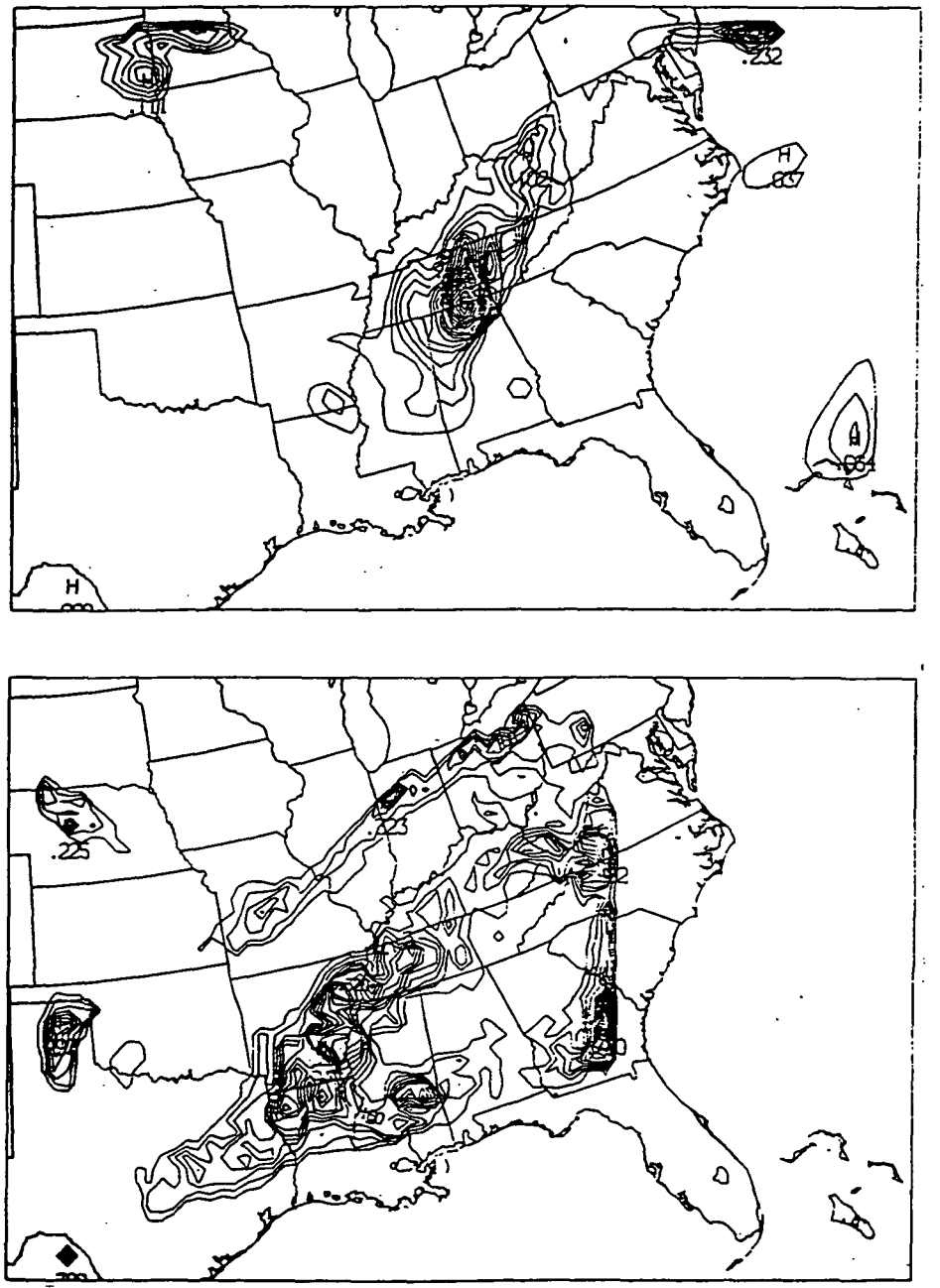

Figure 20 12 h nested MASS convective precipitation forecasts (inches) for 0000 UTC 29 June for the (a) Kuo and (b) Fritsch-Chappell cumulus parameterization schemes.

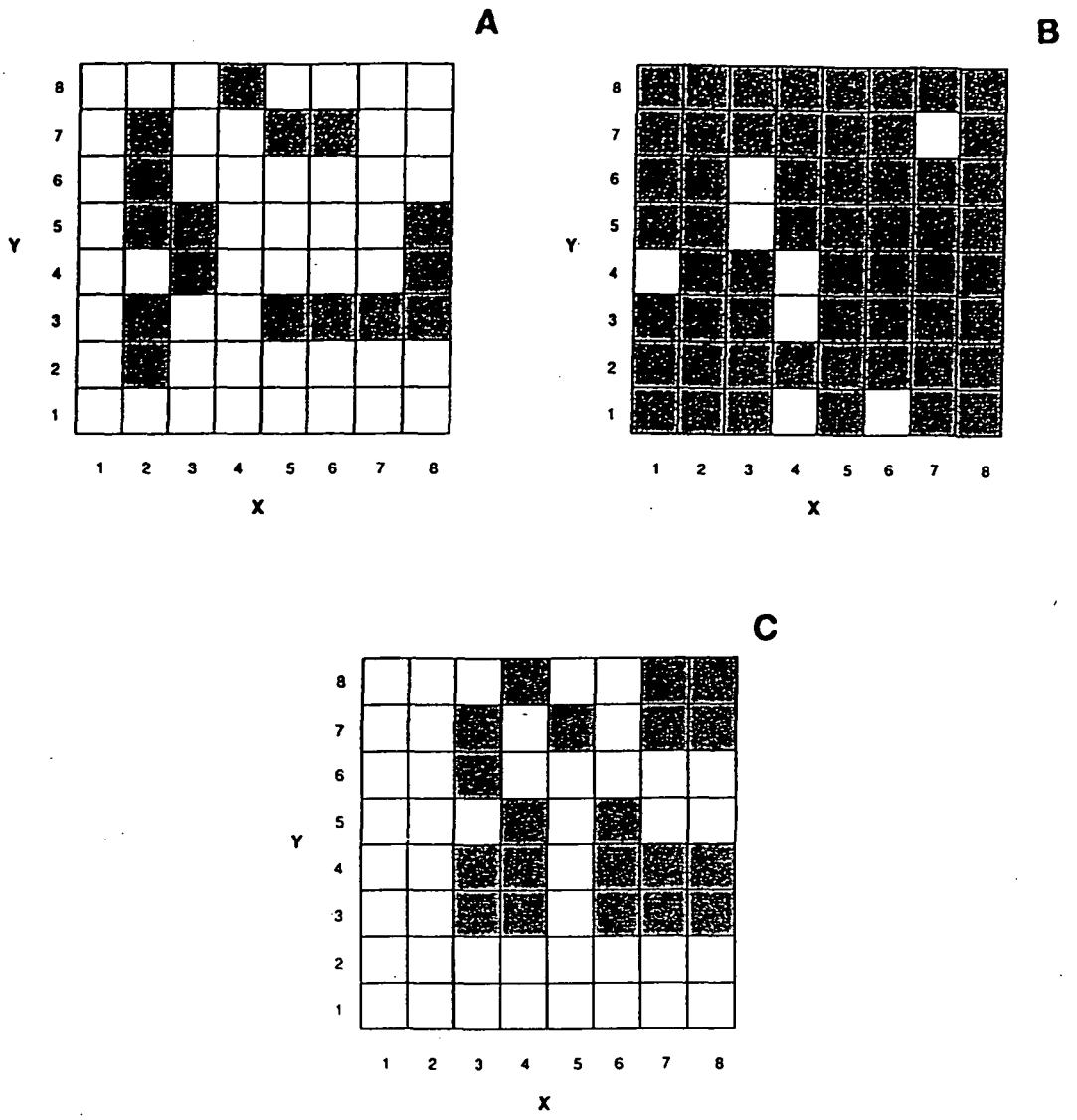

Figure 21 Pattern of mesoscale grid boxes in which the rainfall exceeds 0.1 mm (indicated by shading) from 105 to 135 min: (a) produced by the cloud model, (b) predicted by the Fritsch-Chappell scheme, and (c) predicted by a simple moisture convergence criterion.

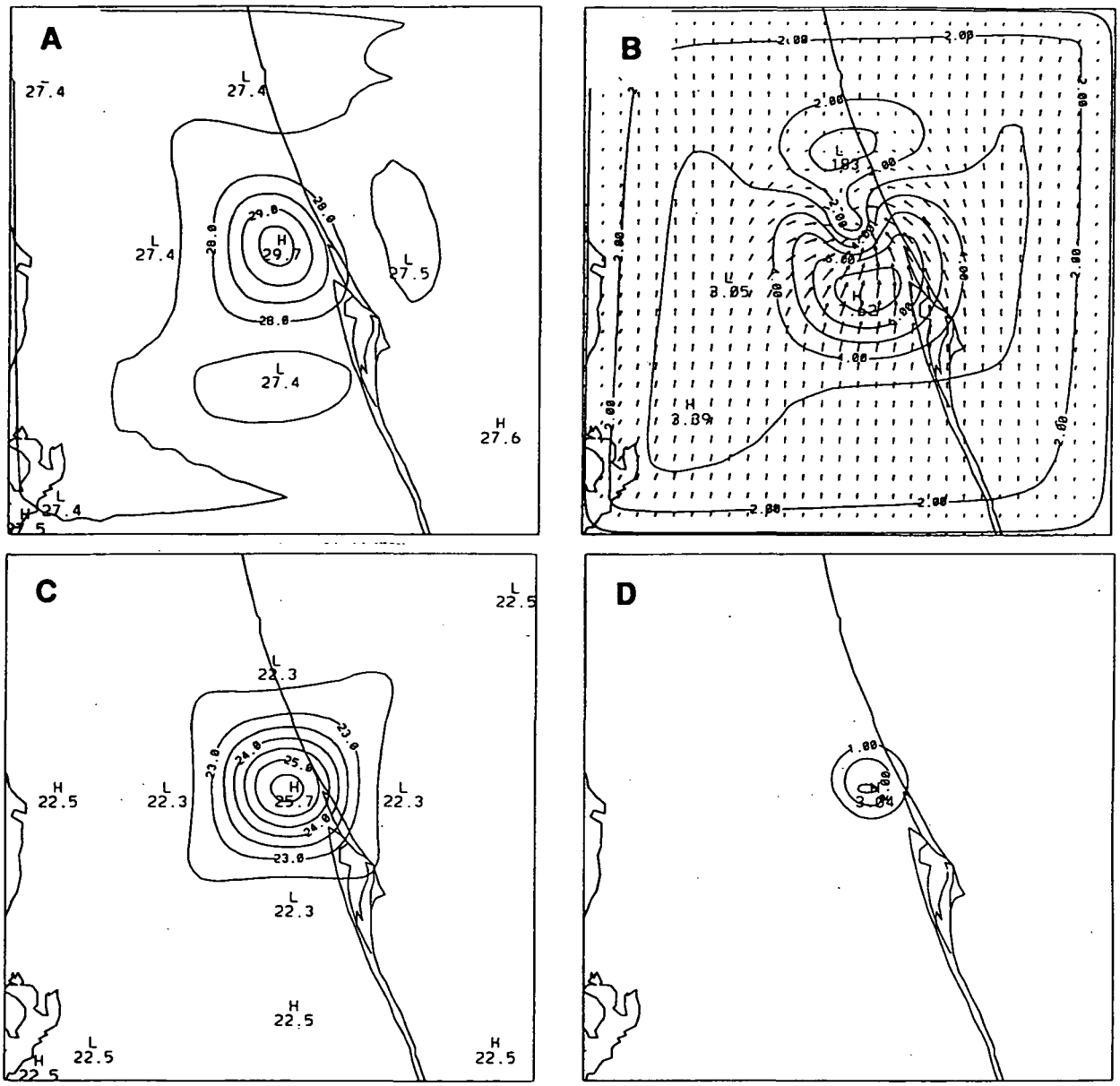

Figure 22 MASS model fields after three hours of simulation using the Kuo cumulus parameterization scheme, with initial and forcing conditions similar to the TASS Florida differential surface heating run. (a)Low level temperature (°C), (b) low level winds, (c) low level dew point (°C), and (d) parameterized convective precipitation (mm). The Florida coastline is drawn; Cape Canaveral is near the center of the domain, and Tampa Bay is in the southwest corner.

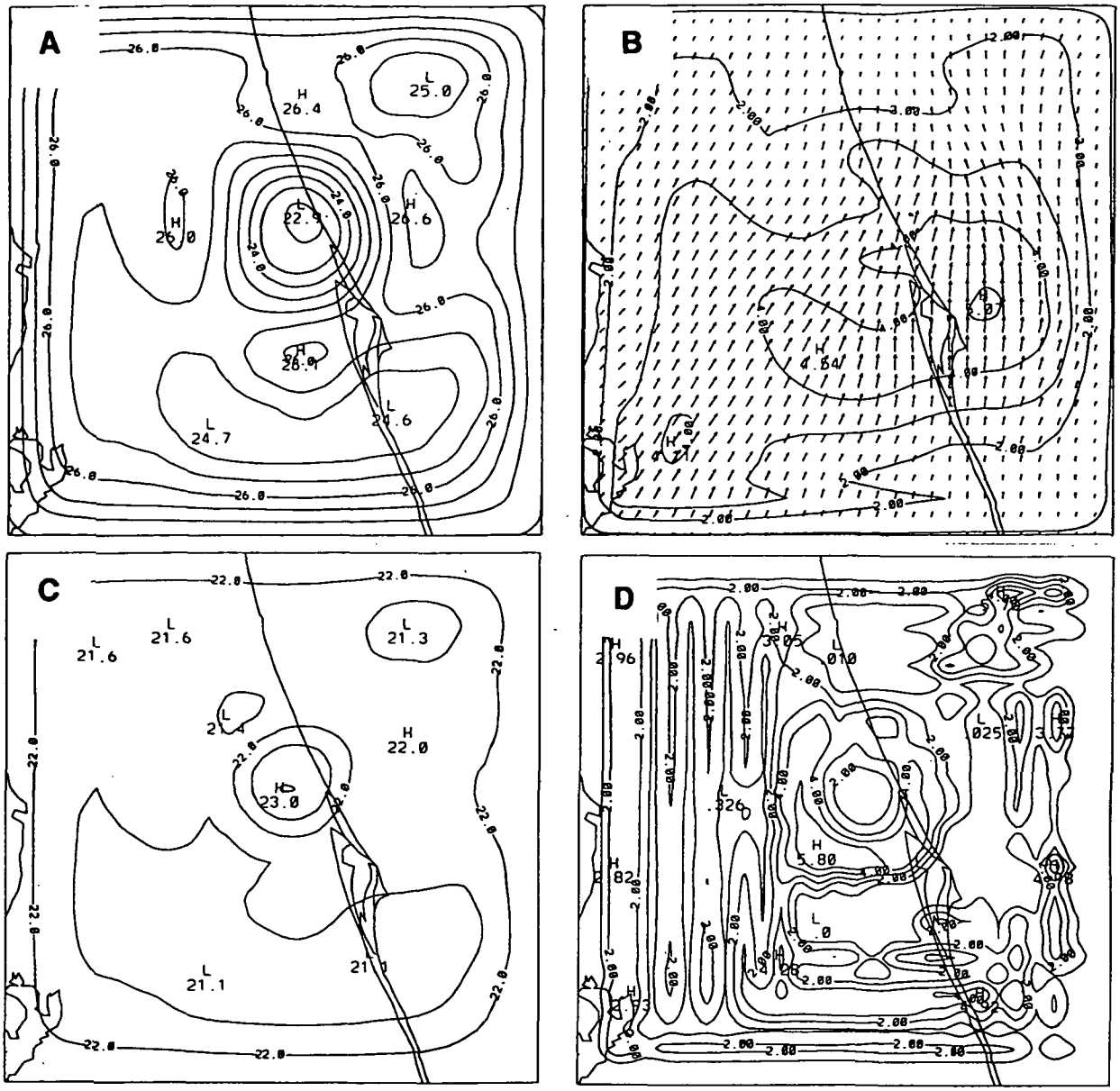

Figure 23 Same as Figure 22 except for a run using the Fritsch-Chappell scheme.

4. Mesoscale/Cloud Scale Model Interaction Studies

The eventual goal of this three year effort was to explore ways to couple mesoscale and cloud scale convective simulations together, after initially using each model independently. Sections 2 and 3 describe independent MASS and TASS efforts; this section will present results from MASS-TASS coupling work. The biggest obstacles to the model interaction studies were the difficulties encountered in mesoscale simulation of the June 28 COHMEX case. In retrospect, it might have been better to have switched to other case studies before getting stalled on that one case, although it is felt that the challenge of the June 28 case is representative of the need for improved techniques in modeling the weakly forced convective environment, and the time invested was well-spent.

4.1 TASS Initial Conditions from MASS

Section 2.3 describes the encouraging results of using nonhomogeneous initial conditions to initiate convection in the TASS model, something that has been done only rarely with three-dimensional cloud models. Low level convergence helped to initiate convection first in the southwest corner of the domain, where thermodynamic instability was at a maximum. A number of technical problems were worked through during that work, among them a change in the lateral boundary condition formulation.

All of the work performed for the COHMEX initial conditions simulations are directly applicable to the problem of initializing TASS with fields interpolated from the MASS model. Two programs were developed, based on earlier MESO work, which would read in a MASS output file of three-dimensional fields and interpolate the data horizontally and vertically to the selected TASS grid. One problem which had to be solved was that the top of the TASS model typically needed to be higher in the atmosphere than the top of the MASS model; the stable stratospheric layer in TASS is important in capping deep convection. An extrapolation method was developed which would produce a simple isothermal layer above the top of the MASS model for the TASS initial state.

The best MASS June 28 simulation was used to test the MASS-TASS coupling technique. A 192 x 192 km box over the COHMEX mesonet was defined. Data for the box was extracted at 2100 UTC 28 June, nine hours into the 37.5 km nested simulation. Fig. 7d shows the convective precipitation field at that time; the convective system which formed in western Tennessee is just moving into the area at the time. The MASS data was then vertically and horizontally interpolated with a cubic spline and placed in a format which could be used for the initialization of a 3 km resolution TASS simulation. The TASS domain covers approximately the same

area covered by the TASS run initialized with meso-β COHMEX data. A test simulation was completed and the output analyzed. Fig. 24 shows the radar reflectivity and low level winds from the simulation superimposed on the observed radar reflectivity at 2300 UTC. The results were disappointing. The TASS simulation did not produce the observed pattern of convection, and the wind field showed problems near the outflow boundary. An analysis of the results indicated that the poor results seemed to be related to the inability of the mesoscale model to reproduce the necessary features of the pre-storm convective environment. In the MASS simulation, the convective system is dying as it enters the COHMEX area; no MASS simulations were obtained which reproduce the strengthening and new generation of convection observed in the COHMEX data (Figs. 3 and 9). Although MASS was able to initiate the original mesoscale convective system in western Tennessee properly, it missed important atmospheric forcing mechanism later in the run.

It was decided that the probability of a successful MASS/TASS coupled simulation would be enhanced if a case with stronger and better-defined mesoscale forcing was used in place of the relatively weak June 28 case. The April 10, 1979 SESAME I case was chosen for this purpose, and original data was obtained. Successful MASS simulations of SESAME case were described in Kaplan *et al.* (1982) and Zack and Kaplan (1987). However, the project ended before a MASS-TASS coupled simulation could be made.

4.2 Nudging TASS Tendencies into MASS

The simplest MASS-TASS nesting approach would be one-way nesting, in which a MASS run provides initial and boundary conditions for a later TASS run, with no TASS information feeding back to the larger scales in the MASS model. In addition to the possibility of using TASS runs at each model grid point instead of a parameterization scheme (Section 3.1), the idea of incorporating averaged tendencies from a TASS run covering a portion of the MASS grid back into the MASS model was explored. The approach taken was to make a MASS run covering an area larger than the Florida differential surface heating TASS run, in which grid points in the MASS model located within the TASS domain would be numerically forced toward time-dependent TASS values. The numerical method was Newtonian relaxation ("nudging"), in which prognostic equations include a term which nudges model variables toward a desired value.

The Florida TASS run uses a 98 x 98 750 m grid, covering an area on the east coast of Florida, northeast of Orlando. The MASS grid is a 30 x 30 10.5 km grid, centered over the TASS area. The resolution of 10.5 km was chosen as an exact multiple of the TASS 73.5 km domain dimension, so that a 14 x 14 grid point box of

TASS grid points are averaged to a single MASS grid point. Values of temperature, water vapor mixing ratio, and u- and v-components of motion in TASS were averaged to MASS grid points every 15 min, beginning 60 min into the 3 h TASS run. For the MASS points covering the TASS domain, the same four prognostic variables were nudged to the TASS variables during a 3 h MASS simulation. The results are shown in Fig. 25. The run can be directly compared to the MASS runs shown in Figs. 22 and 23, which were identical except that conventional cumulus parameterization schemes were used instead of nudging to TASS values.

The nudging simulation produced reasonable results, which compared generally well to the Kuo scheme simulation (Fig. 22). The Kuo scheme's lack of a cool downdraft formulation is apparent. The area of low level heating in the center of the domain is too warm and moist, and the wind field seems to indicate a CISK-type (Conditional Instability of the Second Kind) feedback mechanism which is too strong. The TASS run contained significant cool downdraft activity with some secondary initiation of new cells.

It is encouraging that there were no numerical problems associated with the nudging of the TASS data; for example, there are no sharp gradients near the edges of the TASS data. The nudging technique provides a "gentle" way to introduce outside forcing into the MASS model. It may be useful when full two-way MASS-TASS interaction is achieved.

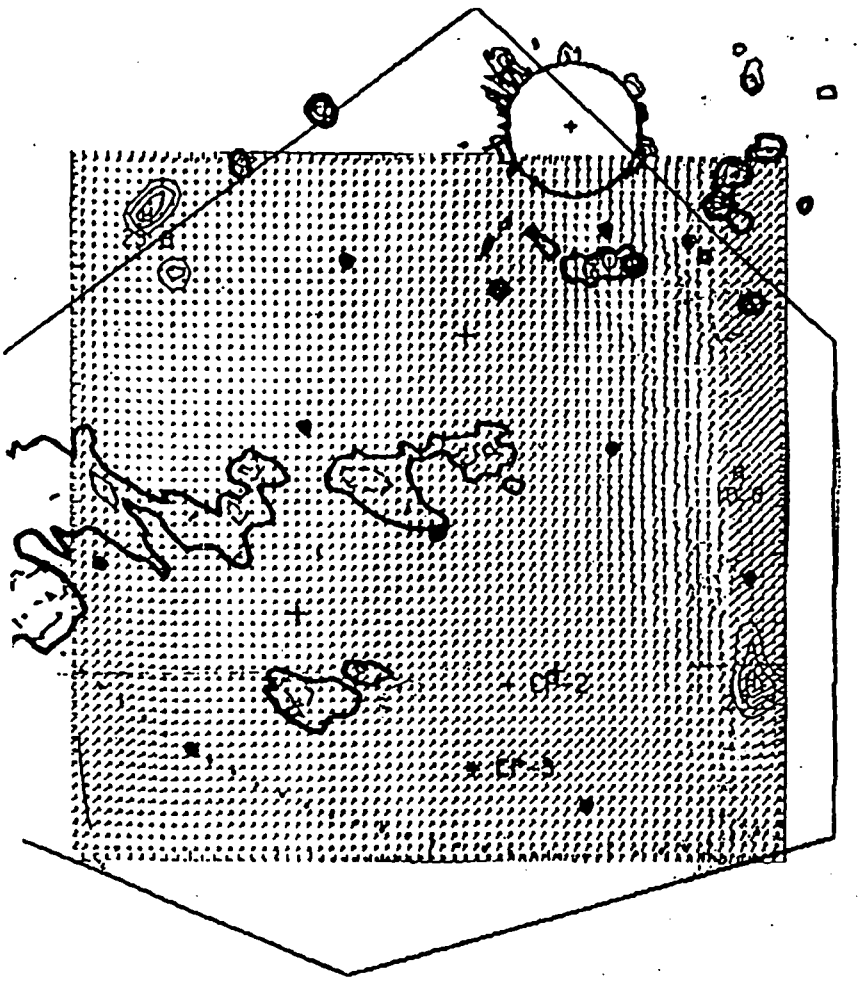

Figure 24 TASS simulated (55 minutes after initialization time) 1 to 4 km mass-weighted radar reflectivity (thin lines, labeled in dBZ) and low level wind vectors superimposed upon the 2300 UTC observed radar reflectivity (unlabeled bold lines).

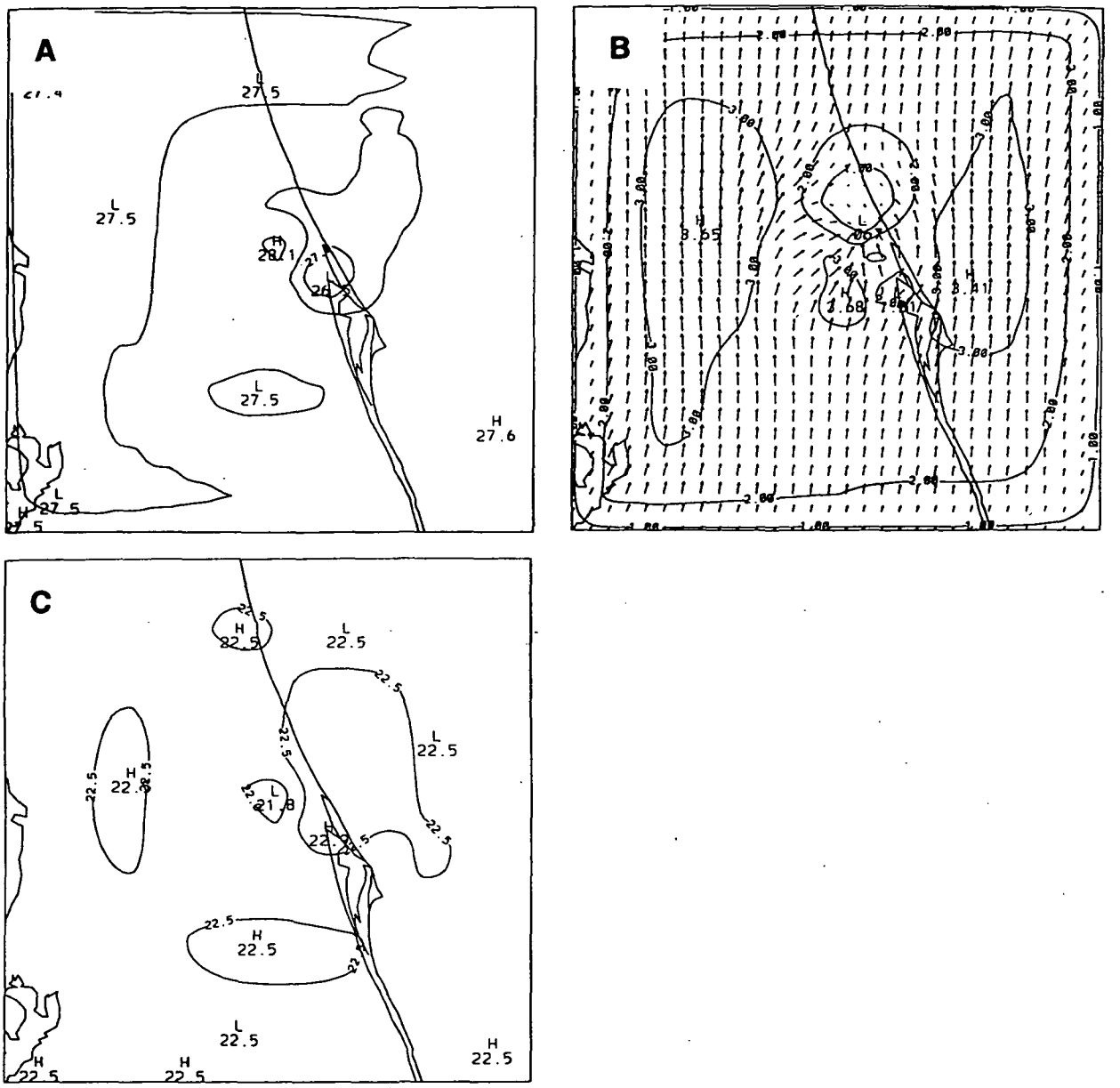

Figure 25 Same as Figure 22 except nudging to TASS simulation results. No convective precipitation field is shown because precipitation was not calculated from TASS.

5. The Future of Convective Simulation

In this section, an attempt is made to summarize the entire project and to explore some of the implications of the research. The difficulties of properly simulating real (as opposed to idealized or theoretical) convection are apparent from the struggles encountered in trying to obtain a satisfactory June 28 mesoscale simulation. The point should again be made that most of the problem stems from the fact that the COHMEX events of June 28-29 occurred in a weakly forced summertime environment, which is generally moist and unstable over a large area; convection was initiated by relatively subtle mechanisms which are typically not resolved by conventional observations. The MASS model and other mesoscale models have had substantial success in parameterizing convection in strongly forced cases, such as the AVE SESAME I (*e.g.* Kaplan, 1982; Kalb, 1985) or the Johnstown flood case (Zhang and Fritsch, 1986a). June 28 represents the kind of convection which occurs almost daily in the warm season over much of the United States, which produces locally significant weather, yet is not predictable by current operational models, or even by current research models. A major conclusion of this project is that for studies of actual (rather than idealized or theoretical) convection, a far better understanding of the initiation process is required. It is felt that initiation has generally been neglected in favor of evolution, and that the ability to successfully forecast thunderstorms depends heavily on progress in the area of initiation.

Much more research is needed to put the pieces of a modeling system together which is capable of significantly improved thunderstorm prediction. The following subsections will suggest the form that such a system might take.

5.1 There's a NEXRAD in Your Future

An important development for the future of convective simulation is the installation of a national Doppler radar network (NEXRAD). Fig. 26 illustrates the regions that will be covered by NEXRAD data by the end of the first phase of installation which was originally scheduled for the end of fiscal 1992 (Fig. 26a) and when the entire system is in place in middle 1990's (Fig. 26b). Thus by the end of the first phase much of the eastern and central United States should be covered with wind data to accuracy of 1 m s^{-1} and a resolution of approximately 1 km. *If the network performs at these anticipated levels, the potential for improvement in local atmospheric simulations should be enormous.*

A recent MESO project involved a preliminary design for a technique to assimilate NEXRAD data into a mesoscale model. A simple Observation System Simulation Experiment (OSSE) was performed to study the effect of incorporating

Doppler data for an idealized case. The algorithm combines the measured radial winds from each Doppler site with model-derived azimuthal winds to compute a three-dimensional wind field. Fig. 27 shows the conventional rawinsonde sites and the planned NEXRAD sites for the chosen area. Fig. 28a shows fields from the surrogate (control) run, along with the same fields for initializations using only the standard (six sites) rawinsonde data (Fig. 28b), rawinsonde and one Doppler site (Fig. 28c), and rawinsonde and all six nearby Dopplers (Fig. 28d). It is clear that for this simple case, the Doppler wind data helps to resolve significant shortwave features which would be missed by the current observational methods.

A national Doppler network in which the data was widely accessible would greatly enhance the ability to effectively initialize fine scale models, especially for nonhydrostatic models. On the meso-γ scale, it is generally true that a knowledge of the wind field is more important than knowledge of the mass field, contrary to the situation for large scale models. It is also likely that the availability of routine Doppler data would further stimulate research on meso-β and meso-γ processes, which would have additional benefits for future modeling efforts.

5.2 Parameterization is Not Dead Yet,

Previous investigators have discussed the relative merits of explicit vs. implicit (parameterized) representations of convection. Molinari and Dudek (1986) found that for hydrostatic models, there is not a length scale below which it is clear that an explicit representation is superior. Zhang *et al.* (1988) suggest that a parameterization scheme is necessary for meso-β models, even with a grid spacing of about 10 km, at the lower limit of application of hydrostatic models. A fundamental difficulty of parameterizing convection with a meso-β scale model is the lack of a clear separation between what is being parameterized and what is being resolved by the model grid. For larger scale models, all convective circulations are clearly subgrid scale and may be parameterized. For cloud models, convection is completely resolved and no parameterization is necessary. In between those two approaches, some parts of the convective circulation may be resolved by mesoscale simulations, while much of the cloud scale circulation is not.

The impressive results of the nonhydrostatic TASS simulations based on two different types of realistic forcing (the three-dimensional COHMEX initialization and the complex surface forcing Florida run) strongly suggest that explicit, nonhydrostatic simulation of convection will ultimately be able to successfully predict convection more accurately than would be possible with the best parameterization scheme. Three barriers are seen which prevent this approach from becoming immediately practical: 1) although computer power is increasing rapidly, cloud model simulations still make extraordinarily large computational

demands, 2) current cloud models (the Colorado State RAMS model may be an exception) generally do not have many of the physical formulations (*e.g.* surface energy budget) necessary for real numerical weather prediction, or the ability to ingest observational data, and 3) observational data to initialize models on the meso-γ scale do not currently exist (but see Section 5.1).

It seems clear, therefore, that convective parameterization in meso-β and larger scale models will still be useful for at least the next five to ten years. Any nonhydrostatic explicit model would still require lateral boundary conditions from a larger scale model. In addition, there is often a significant time lag between what is technically feasible and what is readily available. Sophisticated meso-β scale modeling systems have been used widely in the research community for many years, yet attempts to make such a model operationally useful are relatively new (Golding, 1986; Warner and Seaman, 1990; Zack *et al.*, 1991).

It is believed that substantial progress is still possible for the parameterization approach, especially at the low end of the meso-β scale (10 km). The ability of the TASS model to initiate realistic convection when given realistic forcing mechanisms suggests that a cloud model is currently the best tool available to improve on existing schemes. A cloud model simulation can act as a surrogate atmosphere, in which various parameterization hypotheses may be tested and refined.

One problem inherent to conventional parameterization methods is illustrated in Fig. 29a : one or more convective cells may fall entirely in one mesoscale grid box, while others are split into two or more boxes. In addition, the cells move with time and may propagate from one grid box to another, so that parameterization assumptions may break down. For example, the Fritsch-Chappell scheme (designed for 25 km) assumes that the convective updraft and downdrafts, as well as the compensating environmental vertical motion (primarily subsidence around the periphery of convective cells) all occur in one grid box. This assumption is clearly highly scale-dependent and inadequate for smaller grid sizes.

A new approach is envisioned, in which each convective element is parameterized independently of its location of the mesoscale grid. Instead, an element would be assigned a characteristic size and other features based on mesoscale and subgrid scale variables, then be allowed to be advected by the mesoscale wind field, while being modulated by the changing mesoscale environment. Fig. 29b presents a conceptual picture of the method. Convective tendencies would be calculated in "convective space", a continuous domain of individual convective elements, and then be extrapolated back to the discrete model grid, allowing the convection to be self-scaling, independent of the model resolution

used. That way, different parts of one convective circulation could be assigned to different model grid boxes, which would be advantageous in modeling organized mesoscale convection which could easily span several 10 km grid boxes. Fig. 29b suggests as well a valuable way to analyze cloud model results — by examining averaged cloud model fields over concentric areas (which would not necessarily have to be boxes) centered on an individual or a group of convective elements. An essential advantage of this Lagrangian type of approach would be to avoid the strong dependence of current methods on model grid size.

5.3 The Modeling System of the Future

At the University of Oklahoma's innovative Center for the Analysis and Prediction of Storms (CAPS), two approaches to the model of the future (ARPS, the Advanced Regional Prediction System) are being pursued. The main approach being investigated uses a sophisticated form of grid nesting, called "adaptive mesh refinement". The second possibility is the use of a "dynamic grid adaptation", in which the grid spacing changes in time and in space, responding continuously to changing atmospheric gradients. The idea behind both methods is to obtain high resolution in areas of the grid where it is needed (*e.g.* areas of convection) while avoiding computational expense in more quiescent areas. Many numerical problems would need to be solved before these approaches become operationally useful. The expectation is that new, "massively parallel" computers will eventually provide the necessary computational resources.

Three methods of interaction between MASS and TASS were explored in this project as possible prototypes of future modeling systems. First, a possible configuration would involve the TASS model acting as a replacement for a cumulus parameterization scheme at each model grid point. The divided TASS simulations of Section 3.1 explored this concept, with some technical success, although the computational expense of this approach makes it impractical. A second experiment involved averaging TASS temperature and momentum tendencies to mesoscale grid boxes, and then nudging them directly into MASS, in place of a parameterization scheme (Section 4.2). This method was successful in producing a reasonable, well-behaved MASS simulation, and it represents an intermediate investigative step toward MASS-TASS full two-way interactive nesting.

MESO's ultimate philosophy for effective convective simulation is geared toward the use of TASS simulations nested within a high resolution (10 km) meso-β MASS simulations, although a computer which is affordable for a small company and is capable of running TASS fast enough for anything approaching real time forecasting remains some distance off. For the present, RISC (Reduced Instruction Set Computing) workstation technology has advanced to the point that running

MASS in a real time mode on a 50x40x20 grid can be done on a machine costing less than $100,000. The *Stardent* line of vector-processing workstations provide sufficient number-crunching power, along with sophisticated graphical scientific visualization tools.

Work in several areas will be required (some of which is in progress under other projects) before this can become a reality. First, the June 28 COHMEX case points out several MASS components which need to be improved. Much effort needs to be spent on the surface energy budget, including careful verification with special field experiment data (*e.g.* the First ISLSCP Field Experiment, Sellers *et al.*, 1988). High resolution surface characteristic datasets have become available in recent years; these need to be incorporated routinely into mesoscale simulations. MESO has recently acquired U.S. Geological Survey land use/land cover data and incorporated it into MASS, as well as a 1 km resolution Normalized Difference Vegetation Index (NDVI) dataset on CD-ROM, also from the USGS. These two pieces of information are being used to infer horizontal variations in needed surface properties, such as albedo, ground heat capacity, longwave emissivity and vegetative fraction. The effect of spatial variations of vegetation and soil moisture in modifying a pre-storm environment is discussed by Chang and Wetzel (1991). Since many mesoscale simulations have shown a strong sensitivity to soil moisture, some real time method of estimating soil moisture needs to be developed. This is clearly one of the largest shortcomings of current mesoscale methods. Moisture assimilation from satellite data and other sources needs to be further pursued, because radiative effects from variations in cloud cover can be substantial.

MASS-TASS coupled simulations (Section 4.1) were not very successful in this project. The basic technical capabilities are there, but additional work is needed to make the technique valuable. On the other hand, TASS simulations with observed three-dimensional fields were quite successful, and the Florida TASS simulation with realistic surface forcing was very impressive, inspiring confidence that TASS will produce good results when given good initial data and forcing. Assuming that the mesoscale model can be improved enough to provide good initial conditions for the cloud model, some improvements in the cloud model then become necessary. A scheme which accepts time-dependent lateral boundary conditions from MASS would become necessary. The TASS model does not currently allow for terrain height variations, and it does not have any kind of surface energy budget. These may be necessary for effective cloud scale simulations.

One of the greatest challenges in meteorology is to improve the forecasting of ordinary and severe thunderstorms beyond the standard refrain of "chance of scattered thunderstorms", heard so often in the warm weather months. This project confronted the many difficulties in convective simulation, making significant

progress on both the mesoscale and cloud scale. It is believed that continued research using models of different scales in cooperation, coupled with the continual increase in the availability of powerful computer resources, will result in dramatically better forecasts later in this decade.

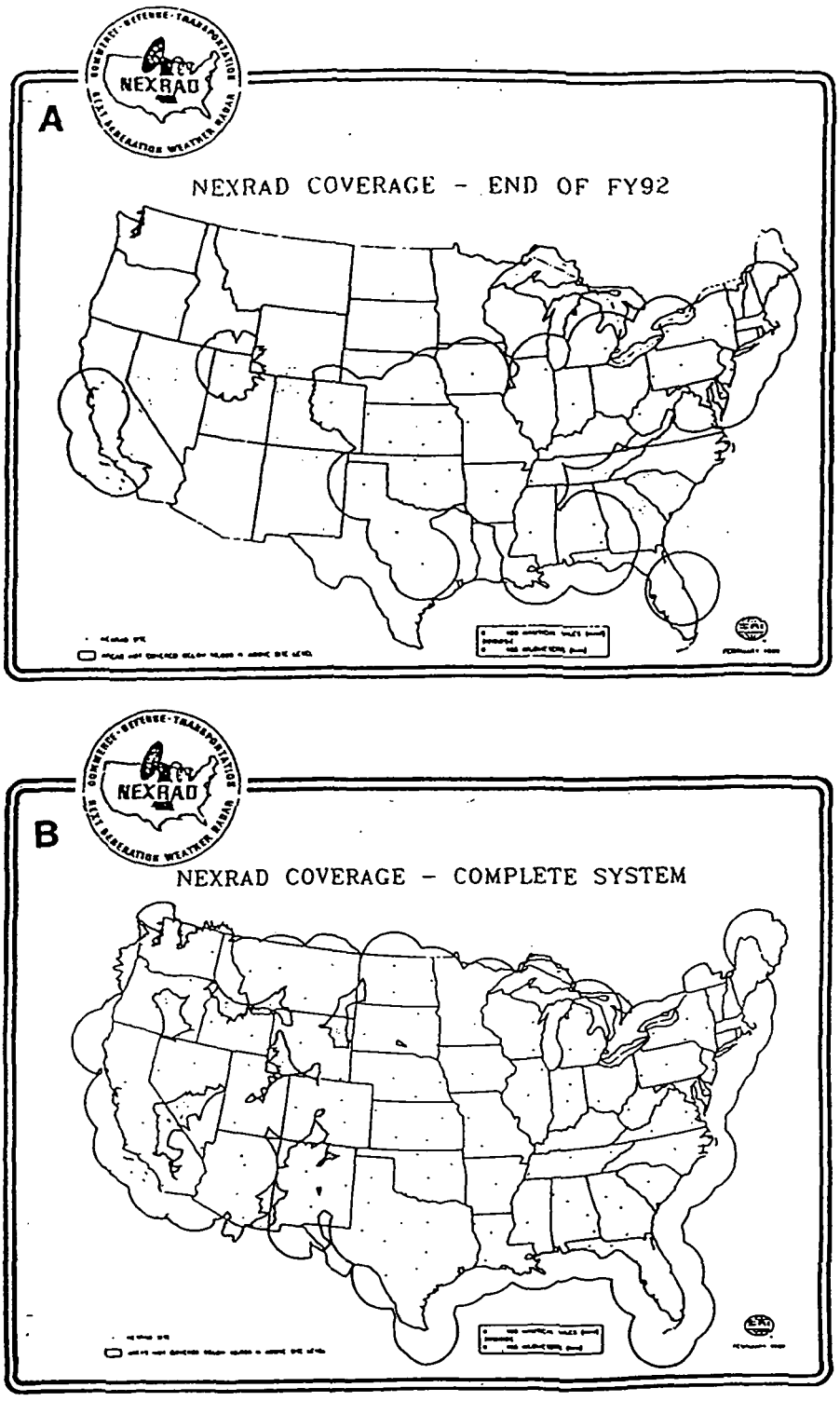

Figure 26 Depiction of the NEXRAD network (a) after the first phase of installation originally scheduled for completion at the end of fiscal 1992 and (b) after the network implementation is complete. The dots depict proposed NEXRAD sites and the circles surrounding each site illustrate the 230 km data radius.

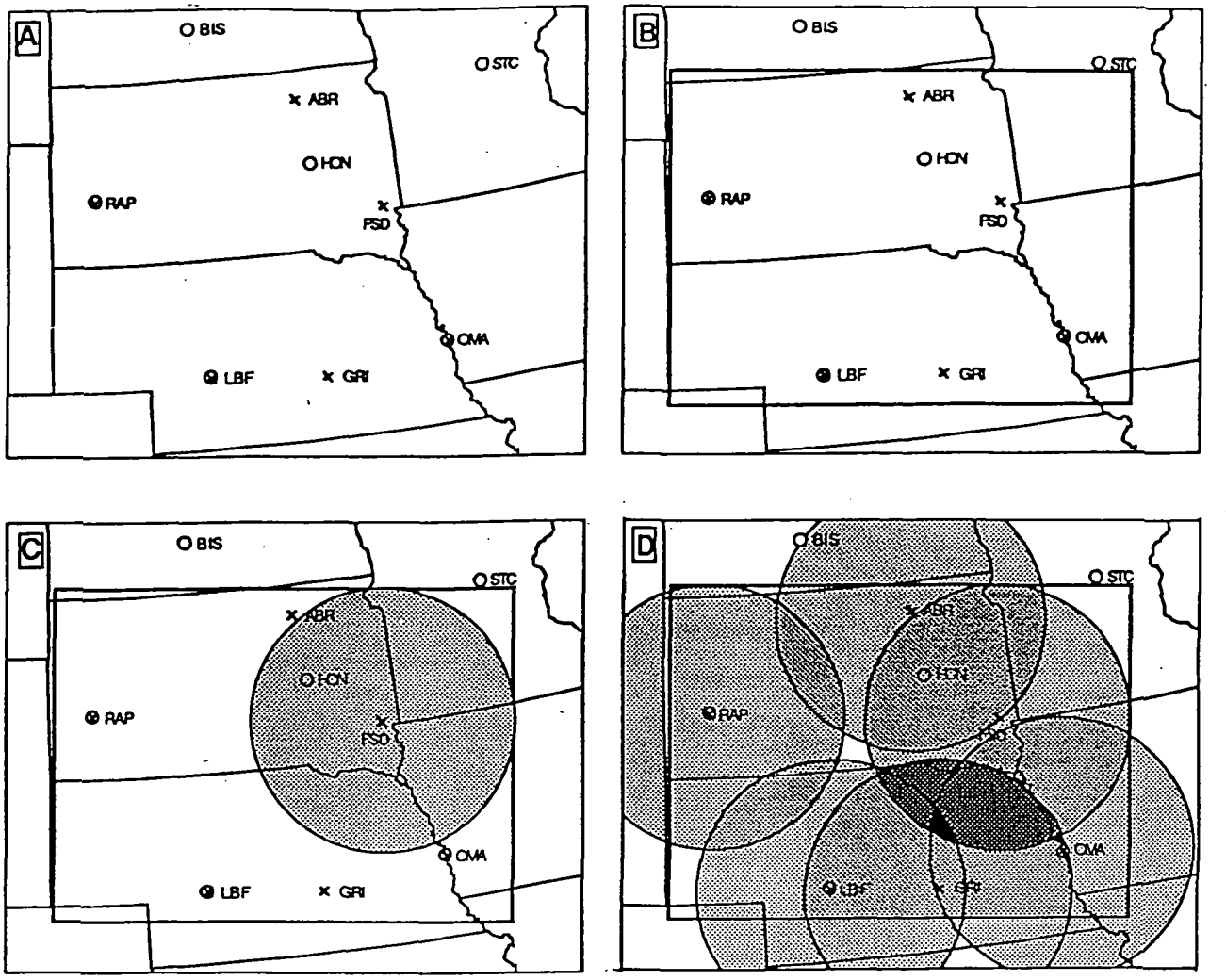

Figure 27 Depiction of the simulation domains and observing sites used in the OSSE: (a) the domain of the surrogate run with circles denoting rawinsonde sites and X's designating Doppler radar sites; (b) same as (a) except the domain of the data assimilation simulations is denoted by the inner rectangle; (c) same as (b) except the radial wind data range of the FSD radar is shaded; (d) same as (c) except the radial wind data ranges of all six radars are shaded, the intensity of the shading is proportional to the number of radars that are capable of providing radial wind data for an area.

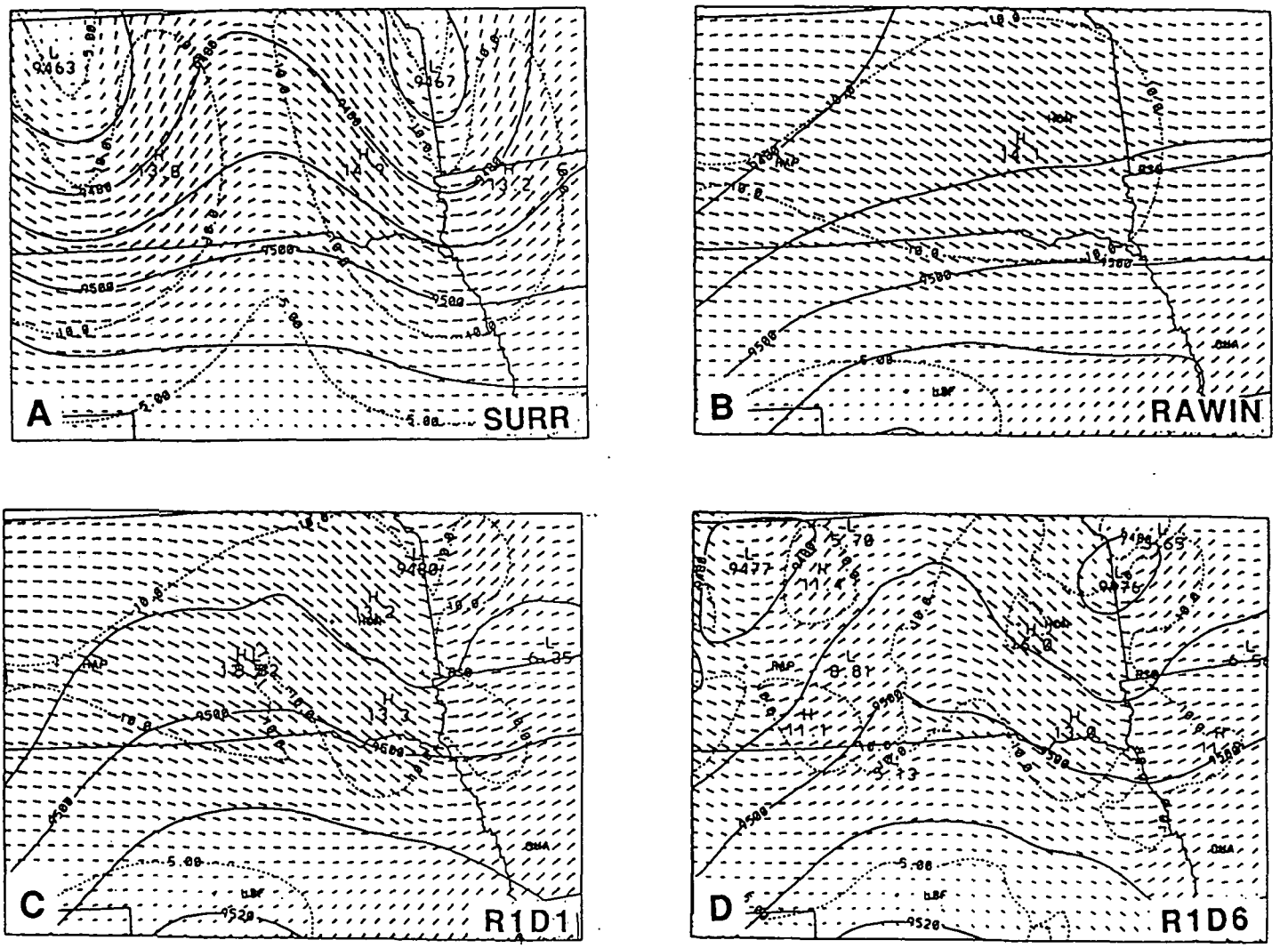

Figure 28 300 mb wind vectors, isotachs (dashed lines, m s^{-1}) and heights (solid lines, m) from the 1200 UTC initialization datasets for (a) surrogate run (SURR), (b) run with only rawinsonde data (RAWIN), (c) rawinsondes with one Doppler radar at Sioux Falls, SD (R1D1), and (d) rawinsondes and six Doppler radars (R1D6).

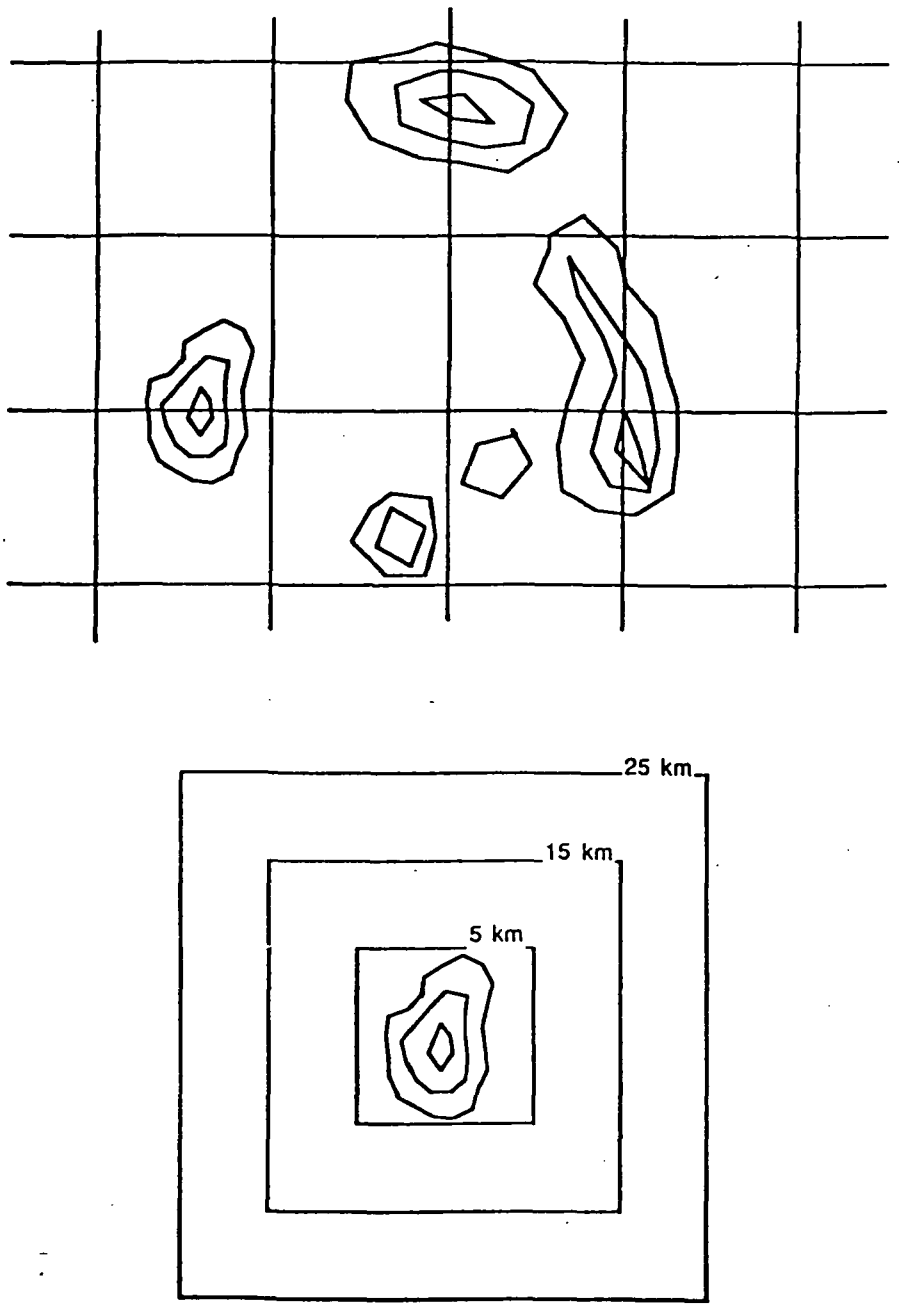

Figure 29 (a) Schematic diagram of the problems encountered in using a fixed grid box method for cumulus parameterization when the size of the grid boxes are comparable to the size of individual convective elements. Some cells overlap boundaries, making theoretical treatment difficult. (b) Proposed alternative method of parameterization, estimating convective effects for a given element or group of elements apart from the particular model grid.

6. Acknowledgements

Over the course of three years, many people contributed to the research effort. The authors gratefully acknowledge the support of Dr. James Dodge of NASA. The research was skillfully guided by Dr. Michael Kalb of USRA. The project was well-conceived and planned by Dr. Michael Kaplan. Dr. Mohan Karyampudi, Dr. Craig Mattocks, Ms. Mary Bousquet, Mr. Glen Coats and Dr. Fred Proctor made significant contributions. Valuable discussions took place with Dr. Pete Robertson of NASA/MSFC and Dr. Kevin Knupp and Dr. Richard McNider of the University of Alabama in Huntsville. Steve Williams, the COHMEX data manager, provided many valuable datasets. The National Climatic Data Center and the National Center for Atmospheric Research, with special help from Mr. Dennis Joseph of NCAR, provided additional data. Computer code and assistance regarding the Fritsch-Chappell scheme was obtained from Dr. Da-Lin Zhang of McGill University, Dr. J. Michael Fritsch of Penn State University and Dr. Kun Gao of NCAR. Substantial computer assistance was provided by Ms. Jayanthi Srikishen of USRA, and Mr. Paul Meyer and Mr. John Parker of NASA/MSFC. Most of the model simulations were carried out on a Cray X/MP 416 at NASA's Marshall Space Flight Center. The discussions of the Florida TASS simulations were based on work performed for the U.S. Air Force Office of Scientific Research under contract F49620-90-C-0057. The NEXRAD Doppler discussion was based on work performed for the New York State Science and Technology Foundation under contract SBIR 90031.

7. References

Anthes, R.A., 1977a: A cumulus parameterization scheme utilizing a one-dimensional cloud model. *Mon. Wea. Rev.*, **105**, 270-286.

_____, 1977b: Hurricane model experiments with a new cumulus parameterization scheme. *Mon. Wea. Rev.*, **105**, 287-300.

Balaji, V. and T.L. Clark, 1988: Scale selection in locally forced convective fields and the initiation of deep cumulus. *J. Atmos. Sci.*, **45**, 3188-3211.

Carbone, R.E., J.W. Conway, N.A. Crook and M.W. Moncrieff, 1990: The generation and propagation of a nocturnal squall line. Part I: Observation and implication for mesoscale predictability. *Mon. Wea. Rev.*, **118**, 26-49.

Chang, J.-T. and P.J. Wetzel, 1991: Effects of spatial variations of soil moisture and vegetation on the evolution of a pre-storm environment: A numerical case study. *Mon. Wea. Rev.*, **119**, 1368-1390.

Chen, C.-H. and H.D. Orville, 1980: Effects of mesoscale convergence on cloud convection. J. Appl. Meteor., **19**, 256-274.

Cooper, H.J., M. Garstang and J. Simpson, 1982: The diurnal interaction between convection and peninsular-scale forcing over South Florida. *Mon. Wea. Rev.*, **110**, 486-503.

Crook, N.A., R.E. Carbone, M.W. Moncrieff and J.W. Conway, 1990: The generation and propagation of a nocturnal squall line. Part II: Numerical simulations. *Mon. Wea. Rev.*, **118**, 50-65.

Frank, W.F., 1983: The cumulus parameterization problem. *Mon. Wea. Rev.*, **111**, 1859-1871.

_____ and C. Cohen, 1987: Simulation of tropical convective systems: Part I: A cumulus parameterization. *J. Atmos. Sci.*, **44**, 3787-3799.

Fritsch, J.M. and C.F. Chappell, 1980: Numerical prediction of convectively driven mesoscale pressure systems. Part I: Convective parameterization. *J. Atmos. Sci.*, **37**, 1722-1733.

Golding, B.W., 1986: Short range forecasting over the United Kingdom using a mesoscale forecasting system. Short and Medium Range Numerical Weather Prediction, ed. Matsuno, Met. Soc. Japan.

Kalb, M.W., 1985: Results from a limited area mesoscale numerical simulation for 10 April 1979. *Mon. Wea. Rev.*, **113**, 1644-1662.

_____, 1987: The role of convective parameterization in the simulation of a Gulf Coast precipitation system. *Mon. Wea. Rev.*, **115**, 214-234.

Kaplan, M.L., J.W. Zack, V.C. Wong and J.J. Tucillo, 1982: Initial results from a mesoscale atmospheric simulation system and comparisons with the AVE-SESAME I dataset. *Mon. Wea. Rev.*, **110**, 1564-1590.

Klemp, J.B., R.B. Wilhelmson and P. Ray, 1981: Observed and numerically simulated structure of a mature supercell thunderstorm. *J. Atmos. Sci.*, **38**, 1558-1580.

Knupp, K.R. and S.F. Williams, 1988: Multiscale analysis of a sustained precipitation event. *Preprints, 12th Conference on Severe Local Storms*, Baltimore, Amer. Meteor. Soc.

Kuo, H.L., 1965: On formation and intensification of tropical cyclones through latent heat release by cumulus convection. *J. Atmos. Sci.*, **22**, 40-63.

_____, 1974: further studies of the parameterization of the influence of cumulus convection on large-scale flow. *J. Atmos. Sci.*, **31**, 1232-1240.

Lafore, J.-P. and M.W. Moncrieff, 1989: A numerical investigation of the scale interaction between a tropical squall line and its environment. *J. Atmos. Sci.*, **46**, 521-544.

Lanicci, J.M., T.N. Carlson and T.T. Warner, 1987: Sensitivity of the Great Plains severe-storm environment to soil-moisture distribution. *Mon. Wea. Rev.*, **115**, 2660-2673.

Lin, Y.-L., R. D. Farley, and H. D. Orville, 1983: Bulk parameterization of the snow field in a cloud model, *J. Climate Appl. Meteor.*, **22**, 1065-1092.

Molinari, J. and M. Dudek, 1986: Implicit versus explicit convective heating in numerical weather prediction models. *Mon. Wea. Rev.*, **114**, 1822-1831.

Mostek, A., and N.W. Junker, 1989: Quantitative precipitation forecast verification at the National Meteorological Center. *Preprints 12th Conference on Weather Analysis and Forecasting*, Monterey, Amer. Meteor. Soc., 633-637.

Ninomiya, K. and K. Kurihara, 1987: Forecast experiment of a long-lived meso-α-scale convective system in Baiu frontal zone. *J. Met. Soc. Japan*, **65**, 885-899.

Ookouchi, Y., M. Segal, R.C. Kessler and R.A. Pielke, 1984: Evaluation of soil moisture effects on the generation and modification of mesoscale circulations. *Mon. Wea. Rev.*, **112**, 2281-2292.

Proctor, F.H., 1987a: The Terminal Area Simulation System. Volume I: Theoretical formulation, NASA CR-4046.

_____, 1987b: The Terminal Area Simulation System. Volume II: Verification Cases, NASA CR-4047.

Redelsperger, J.-L. and T.L. Clark, 1990: The initiation and horizontal scale selection of convection over gently sloping terrain. *J. Atmos. Sci.*, **47**, 516-541.

Rutledge, S. A. and P. V. Hobbs, 1983: The mesoscale and microscale structure and organization of clouds and precipitation in midlatitude cyclones. VIII: A model for the "seederfeeder" process in warm-frontal rainbands, *J. Atmos. Sci.*, **40**, 1185-1206.

Schlesinger, R.E., 1982: Effects of mesoscale lifting, precipitation and boundary layer shear on severe storm dynamics in a three-dimensional numerical modeling study. *Preprints, 12th Conference on Severe Local Storms*, San Antonio, Amer. Meteor. Soc., 536-541.

Sellers, P.J., F.G. Hall, G. Asrar, D.E. Strebel and R.E. Murphy, 1988: The First ISLSCP Field Experiment (FIFE). *Bull. Amer. Meteor. Soc.*, **69**, 22-27.

Song, J.A. and M.L. Kaplan, 1991: Observation and numerical simulation of a convective initiation during COHMEX. *To be submitted as a NASA Technical Memorandum.*

Tripoli, G.J. and W.R. Cotton, 1989a: A numerical study of an observed orogenic mesoscale convective system. Part I: Simulated genesis and comparison with observation. *Mon. Wea. Rev.*, **117**, 273-304.

_____, and _____, 1989b: A numerical study of an observed orogenic mesoscale convective system. Part II: Analysis of governing dynamics. *Mon. Wea. Rev.*, **117**, 305-328.

Waight, K.T., J.W. Zack and V.M. Karyampudi, 1989: The need for enhanced initial moisture information in simulations of a complex summertime precipitation event. *Preprints, 12th Conference on Weather Analysis an Forecasting*, Monterey, Amer. Meteor. Soc., 121-124.

Wang, W. and T.T. Warner, 1988: Use of four-dimensional data assimilation by Newtonian relaxation and latent-heat forcing to improve a mesoscale-model precipitation forecast: A case study. *Mon. Wea. Rev.*, **116**, 2593-2613.

Warner, T.T. and N.L. Seaman, 1990: A real-time, mesoscale numerical weather-prediction system used for research, teaching and public service at The Pennsylvania State University. *Bull. Amer. Meteor. Soc.*, **71**, 792-805.

Williams, S.F., H.M. Goodman, K.R. Knupp and J.E. Arnold, 1987: SPACE/COHMEX Data Inventory Document. NASA TM-4006, Marshall Space Flight Center, AL, 480 pp.

Wolcott, S.W. and T.T. Warner, 1981: A moisture analysis procedure utilizing surface and satellite data. *Mon. Wea. Rev.*, **109**, 1989-1998.

Yoshizaki, M. and Y. Ogura, 1988: Two- and three-dimensional modeling studies of the Big Thompson storm. *J. Atmos. Sci.*, **45**, 3700-3722.

Zack, J.W. and M.L. Kaplan, 1987: Numerical simulations of the subsynoptic features associated with the AVE_SESAME I case. Part I: The preconvective environment. *Mon. Wea. Rev.*, **115**, 2367-2394.

_____, V.M. Karyampudi, C.A. Mattocks and G.D. Coats, 1988: Meso-beta scale simulations of convective cloud systems over Florida utilizing synthetic data derived from GOES satellite imagery. *Preprints, Eighth Conference on Numerical Weather Prediction*, Baltimore, Amer. Meteor. Soc.

_____, C.A. Mattocks and M.D. Bousquet, 1991: A statistical-dynamical mesoscale thunderstorm forecast system for the Kennedy Space Center. *Preprints, Ninth Conference on Numerical Weather Prediction*, Denver, Amer. Meteor. Soc.

Zhang, D.-L., E.-Y. Hsie and M.W. Moncrieff, 1988: A comparison of explicit and implicit predictions of convective and stratiform precipitating weather systems with a meso-β-scale numerical model. *Quart. J. Roy. Meteor. Soc.*, **114**, 31-60.

_____, K. Gao and D.B. Parsons, 1989: Numerical simulation of an intense squall line during 10-11 June 1985 PRE-STORM. Part I: Model verification. *Mon. Wea. Rev.*, **117**, 960-994.

_____, and J.M. Fritsch, 1986a: Numerical simulation of the meso-β-scale structure and evolution of the 1977 Johnstown flood. Part I: Model description and verification. *J. Atmos. Sci.*, **43**, 1913-1943.

_____, and _____, 1986b: A case study of the sensitivity of numerical simulation of mesoscale convective systems to varying initial conditions. *Mon. Wea. Rev.*, **114**, 2418-2431.

_____, and _____, 1988: A numerical investigation of a convectively generated, inertially stable, extratropical warm-core mesovortex over land. Part I: Structure and evolution. *Mon. Wea. Rev.*, **116**, 2660-2687.